nagra.

Arbeitsbericht NAB 21-03

Development of analytical methods for the detection of ^{14}C-bearing carbon compounds at ultra-low concentrations

January 2021

T. Guillemot, B.Z. Cvetković, D. Kunz,
G. Salazar, M. Rauber, S. Szidat & E. Wieland

National Cooperative
for the Disposal of
Radioactive Waste

Hardstrasse 73
P.O. Box 280
5430 Wettingen
Switzerland
Tel. +41 56 437 11 11

www.nagra.ch

nagra.

Arbeitsbericht NAB 21-03

Development of analytical methods for the detection of ^{14}C-bearing carbon compounds at ultra-low concentrations

January 2021

T. Guillemot[1], B.Z. Cvetković[1], D. Kunz[1], G. Salazar[2], M. Rauber[2], S. Szidat[2] & E. Wieland[1]

[1] Paul Scherrer Institute
[2] University of Berne, Department of Chemistry and Biochemistry & Oeschger Center for Climate Change Research

KEYWORDS

Carbon-14; carbon compounds; ion and gas chromatography; accelerator mass spectrometry; corrosion; irradiated steel

National Cooperative for the Disposal of Radioactive Waste

Hardstrasse 73
P.O. Box 280
5430 Wettingen
Switzerland
Tel. +41 56 437 11 11

www.nagra.ch

Nagra Arbeitsberichte ("Working Reports") present the results of work in progress that have not necessarily been subject to a comprehensive review. They are intended to provide rapid dissemination of current information.
This report was prepared on behalf of Nagra. The viewpoints presented and conclusions reached are those of the author(s) and do not necessarily represent those of Nagra.

Abstract

Carbon-14 (^{14}C) is an important, dose-contributing radionuclide released during corrosion of irradiated steel components in a deep geological repository. For a repository for low- and intermediate-level radioactive waste (L/ILW), the contribution of ^{14}C to the dose may be dominant. Since speciation is a key parameter with respect to transport resp. retention, knowledge about the speciation of ^{14}C-bearing carbon compounds is essential to support future safety assessments for an L/ILW repository. To this end, a unique corrosion experiment with irradiated steel is currently running at the Paul Scherrer Institute, which required the development of very sensitive analytical techniques for the identification and quantification of ^{14}C-bearing carbon compounds at ultra-low concentrations. The analytical approach was based on ^{14}C quantification by accelerator mass spectrometry (AMS) as it was expected that the concentrations of the ^{14}C-bearing carbon compounds might be extremely low due to the low ^{14}C inventory of the irradiated steel used for the corrosion experiment and the very low corrosion rate of steel in strongly alkaline conditions.

Analytical methods based on compound-specific radiocarbon analysis (CSRA) were developed for single compounds by combining chromatographic separation of the carbon compounds with either high performance ion chromatography in the case of aqueous species or gas chromatography in the case of gaseous species, respectively, and ^{14}C quantification by AMS. CSRA allows single aqueous and gaseous ^{14}C-bearing carbon compounds to be identified and quantified at the pico- to femto-molar concentration level. In addition, AMS-based analytical methods for the determination of the total organic and inorganic ^{14}C contents in solution (organic: $TO^{14}C$ and inorganic: $TI^{14}C$) as well as the total ^{14}C content in the gas phase ($TG^{14}C$) were developed.

Development of the aforementioned methods is documented in this report. The methods were tested by using ^{14}C standards in order to determine their recovery rate, verify reproducibility and quantify efficiency of the involved processes and devices. After validation of the AMS-based analytical methods, they were applied to quantify the ^{14}C-bearing carbon compounds present in the liquid and gas phases after more than 3 years of corrosion of irradiated steel. The results show that ^{14}C is predominantly associated with organic carbon compounds in the liquid phase, while the amount of ^{14}C bound by inorganic carbon is significantly lower. CSRA further revealed that acetic, formic, lactic, malonic, and oxalic acids are important ^{14}C-bearing carbon compounds in the liquid phase. $^{14}CH_4$ and $^{14}C_2H_6$ were the ^{14}C-bearing compounds identified in the gas phase. The former hydrocarbon is the main ^{14}C-carrying gaseous species as it contributes ~ 90 % to $TG^{14}C$.

Table of Contents

List of Tables

List of Figures

List of Abbreviations

^{14}C	Carbon-14
a	annum
AA	Acetic Acid
ACW	Artificial Cement pore Water
AMS	Accelerator Mass Spectrometry
API	Atmospheric Pressure Ionisation
a.u.	arbitrary unit
CAs	Carboxylic Acids
CSRA	Compound-Specific Radiocarbon Analysis
d-TO^{14}C	Direct measurement of Total Organic ^{14}C
EA	Elemental Analyser
ESI	negative ElectroSpray Ionisation
FA	Formic Acid
F^{14}C	Fraction of modern carbon
GA	Glycolic Acid
GC	Gas Chromatography
GIS	Gas Interface System
HCs	Hydrocarbons
HPIEC	High Performance Ion Exchange Chromatography
IC	Ion Chromatography
i.d.	inner diameter
L/ILW	Low- and Intermediate-Level Waste
LA	Lactic Acid
LARA	Laboratory for the Analysis of Radiocarbon
LC	Liquid Chromatography
LOD	Limit of Detection
LOQ	Limit of Quantification
LSC	Liquid Scintillation Counting
MA	Malonic Acid
MICADAS	MIni CArbon DAting System
MS	Mass Spectrometry

n.d.	not determined
NDIR	Non-Dispersive Infrared Detector
NPOC	Non-Purgeable Organic Carbon
OA	Oxalic Acid
o.d.	outer diameter
p-TO^{14}C	Total Organic ^{14}C after solution pre-treatment with cartridge
SIM	Selected Ion Monitoring
TCD	Thermal Conductivity Detector
TI^{14}C	Total Inorganic ^{14}C
TG^{14}C	Total Gaseous ^{14}C
TO^{14}C	Total Organic ^{14}C

1 Introduction

Carbon-14 (^{14}C) is an important, dose-contributing radionuclide released from radioactive waste (e.g. Johnson & Schwyn 2008, Nagra 2002, 2016, NDA 2012, Yim & Caron 2006). ^{14}C has a long half-life (5'730 a), its gaseous and aqueous organic species have a high mobility in the repository system and its environment, and it can be incorporated in the human food chain. The speciation of ^{14}C-carrying carbon compounds, their rate of release from waste materials and their paths of migration in the near field, host rock and access structures have to be taken into account in safety assessments for a deep geological repository, mainly for low- and intermediate-level waste (L/ILW). ^{14}C in its organic chemical forms, both as gaseous and aqueous species, may contribute to and even dominate dose release from an L/ILW repository. The inorganic forms (e.g. CO_2, HCO_3^- and CO_3^{2-}) should be strongly retarded in the cementitious near field of the L/ILW repository by precipitation as calcium carbonate or isotopic exchange with stable CO_3^{2-} (e.g. Allard et al. 1981, Bayliss et al. 1988, Pointeau et al. 2003). Therefore, they have only a negligible effect on dose release.

In Switzerland, the main source of ^{14}C in the already existing and future arising L/ILW is irradiated steel (~ 75 %) (Johnson & Schwyn 2008, Nagra 2014). ^{14}C is generated by the activation of nitrogen (N) impurities contained in metallic waste components from the decommissioning of nuclear power plants according to the nuclear reaction $^{14}N(n,p)^{14}C$. Corrosion of the irradiated steel components will occur upon disposal in the planned L/ILW repository and give rise to the release of ^{14}C as dissolved and/or gaseous compounds.

At the Paul Scherrer Institute (PSI), the corrosion of irradiated steel is currently being investigated in a gas-tight reactor under anoxic, alkaline conditions. The experiment was started in May 2016 and since then, the liquid and gas phases have regularly been sampled (Cvetković et al. 2018a). According to scoping calculations carried out prior to starting the experiment, extremely low ^{14}C concentrations are anticipated in the reactor for several reasons: i) the irradiated steel used for the experiment has a relatively low ^{14}C inventory (Schumann et al. 2014); ii) the corrosion of stainless steel in alkaline conditions is extremely slow (Diomidis 2014, Smart 2009, Smart et al. 2002, Swanton et al. 2015); and iii) only limited volumes can be sampled from the reactor. Thus, these constraints required the development of a very sensitive analytical technique based on ^{14}C accelerator mass spectrometry (AMS) measurements. The detection of ^{14}C by AMS is much more sensitive than detection by the standard decay counting method (i.e. liquid scintillation counting, LSC) and allows the determination of the $^{14}C/^{12}C$ isotopic ratio in the concentration range from 10^{-12} to 10^{-16} g/L (Turteltaub & Vogel 2000). For the present study, the ^{14}C measurements were carried out with the MICADAS (MIni CArbon DAting System) operated by the Laboratory for Analysis of Radiocarbon (LARA) at the University of Berne (Szidat et al. 2014). A compound-specific radiocarbon analysis (CSRA) method based on chromatographic separation techniques in combination with ^{14}C quantification by AMS was developed to quantify individual ^{14}C-bearing organic compounds present in solution and gas phase. CSRA for gaseous carbon compounds is novel and described for the first time in this report. The formation of ^{14}C-bearing hydrocarbons (HCs) was expected based on the results from batch-type experiments carried out with non-irradiated zero-valent iron powders in anoxic alkaline conditions (Cvetković et al. 2018b). The current development was based on the assumption that stable carbon bound in iron and ^{14}C bound in irradiated steel might have similar chemical speciation and reactivity.

This report describes the development and optimisation of the analytical methods employed for the identification and quantification of stable carbon and ^{14}C-bearing carbon compounds released to solution and gas phase during the corrosion of irradiated steel. Determination of the ^{14}C speciation comprises dissolved ^{14}C-bearing carbon compounds, the total organic ^{14}C content ($TO^{14}C$) of the solution, the total inorganic ^{14}C content of the solution ($TI^{14}C$), the gaseous ^{14}C-bearing HCs and the total ^{14}C content of the gas phase ($TG^{14}C$).

2 Corrosion experiment with irradiated steel

2.1 Layout

The corrosion experiment with irradiated steel uses two 1 g specimens prepared from an irradiated steel nut. The irradiated steel nuts were obtained from the nuclear power plant (NPP) of Gösgen (Switzerland). They are immersed in artificial cement pore water (ACW) at pH 12.5 inside a gastight autoclave-type reactor (Fig. 1). They were exposed to radiation for about two years (Schumann et al. 2014). The ^{14}C activity was determined experimentally by wet chemistry digestion combined with LSC and found to be 17.8 ± 2.5 kBq per gram, which corresponds to a ^{14}C content of 0.107 ± 0.015 µg/g. Details about the composition of the steel nuts and the analytical methods were reported by Schumann et al. (2014).

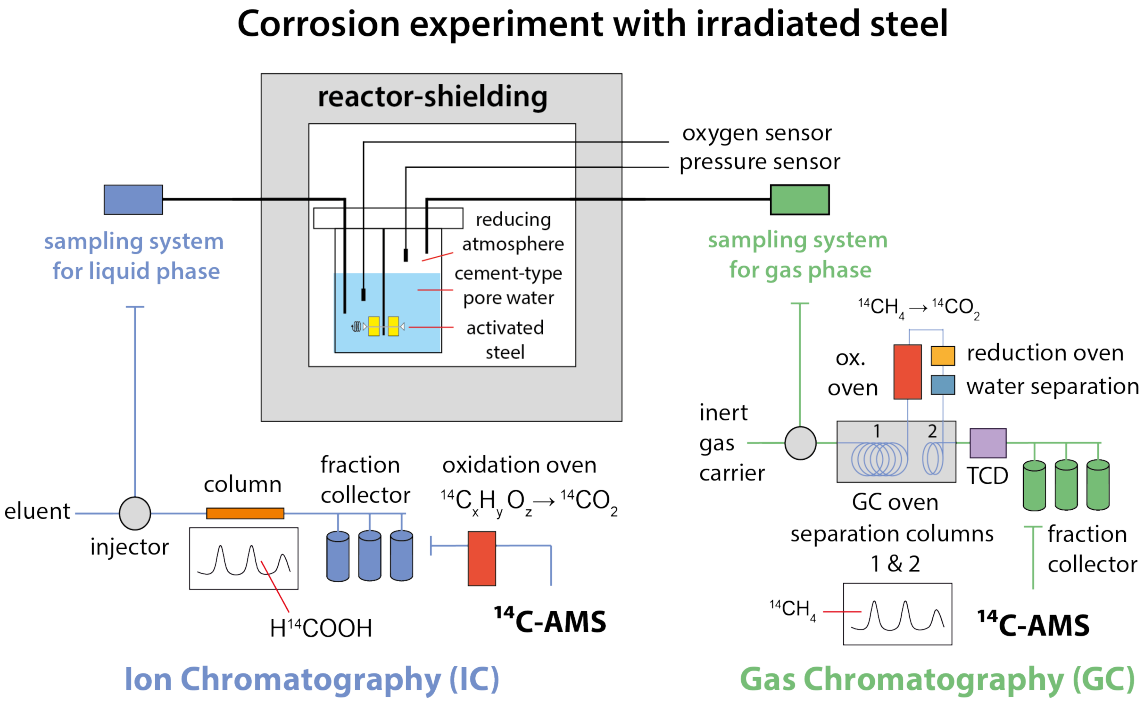

Fig. 1: Representation of the corrosion experiment with irradiated steel

It includes the set-up of the reactor and the schematics of the methods developed for analysing the liquid and gas phases sampled from the reactor.

The reactor contains 300 mL ACW solution and has a gas volume of 200 mL. The ACW solution is prepared in a glove box under controlled N_2 atmosphere (O_2 and CO_2 < 0.1 ppm) with "O_2-free", ultrapure water (see Section 3.1). It is injected into the reactor using the in-house developed sampling system and N_2 overpressure. The gas phase is composed of N_2 to maintain anoxic conditions and kept at an overpressure of 4 bar to facilitate the sampling. The operational conditions of the reactor are constantly monitored by measuring pressure, temperature, and concentration of dissolved O_2 in solution (Fig. 1). Until now, the collection of liquid and gas samples has been carried out at days 0, 1, 14, 28, 92, 286, 412, 552, 1'114, and 1'252 of the reaction.

2.2 Sampling

For the sampling of the liquid phase, a 7 mL sampling tube made of stainless steel and equipped with two valves at the in- and outlet was connected to the liquid outlet valve of the reactor (Wieland et al. 2017). The tube was purged at least three times with N_2 and evacuated. By opening the valves between the reactor and the evacuated sampling tube, the liquid phase was pressed from the reactor into the tube as a result of the N_2 overpressure. Afterwards, the tube was closed, disconnected from the reactor, and transferred into a glove box with N_2 atmosphere. The tube was weighed before and after sampling to determine the exact volume of the solution.

The gas phase was collected with a 50 mL gas sampling tube connected to the gas outlet of the reactor (Wieland et al. 2017). The gas sampling tube was purged at least three times with N_2 and then evacuated. By opening the valves in between the reactor and the tube, around 50 mL from the gas phase of the reactor were collected. At the end of the sampling procedure, the volume of the liquid phase was adjusted in the reactor by adding 7 mL "O_2-free" fresh ACW via the sampling tube with the help of applied N_2 overpressure. If the gas pressure was below 4 bar overpressure after the injection of fresh ACW solution, N_2 was added to maintain the initial operational conditions in the reactor.

3 Analytical methods and developments

3.1 Solutions and chemicals

Throughout this study, the solutions were prepared using Fluka or Merck analytical grade ("pro analysis") chemicals. Ultrapure (deionised, de-carbonated) water (Milli-Q® water; 18.2 MΩ cm resistance) generated by a Milli-Q gradient A10 purification system (Merck Millipore, Burlington, MA, USA) was used for the preparation of solutions and sample dilution. Degassed O_2-free water was prepared by boiling the ultrapure water for two hours under continuous N_2 purge. The O_2 concentration was controlled with a PreSens PSt6 planar oxygen sensor (Regensburg, Germany), which recorded a value below 1 ppb, corresponding to the limit of detection. All wet chemistry experiments were carried out in glove boxes under a controlled N_2 atmosphere (O_2 and CO_2 < 0.1 ppm).

The composition of the ACW solution corresponded to a pore solution at pH 12.5 in equilibrium with respect to portlandite during the second stage of the cement degradation. For the preparation of the solution, $CaCO_3$ was heated at 1'000 °C until constant weight, producing CaO. 2 g CaO was added to 1'000 mL degassed ultrapure water and equilibrated for two days under a N_2 atmosphere by using an end-over-end shaker. After 14 h, the solution was filtered through 100 nm polyethersulfone membrane filters (Criticap-M™, Gelman Sciences Inc., East Lansing, MI, USA) and stored in the glove box until further use.

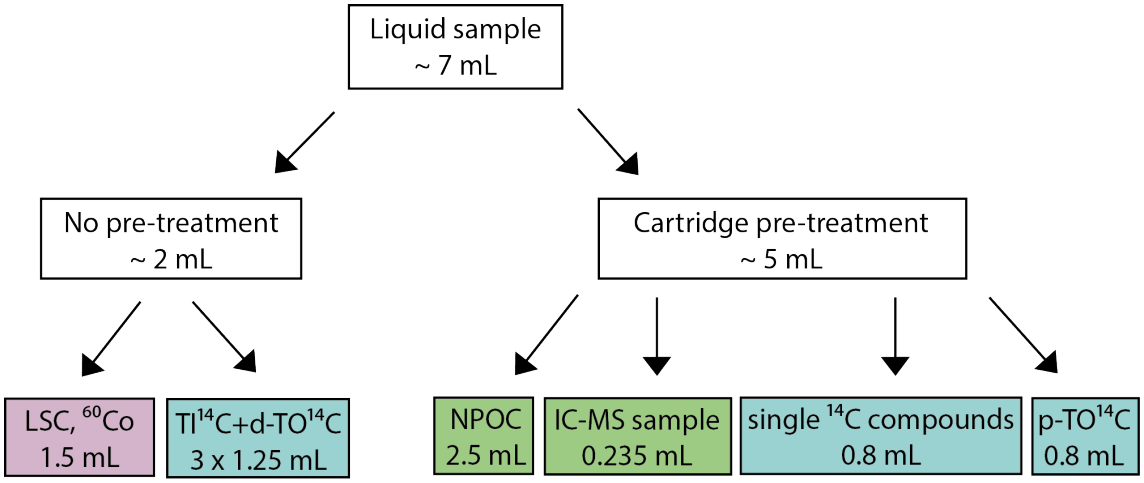

Fig. 2: Scheme of the analytical protocol of the aqueous samples

In green: stable carbon analyses, in blue: AMS analyses, in purple: radio analysis. The $TO^{14}C$ content was determined in two different ways: d-$TO^{14}C$ refers to the direct measurement of $TO^{14}C$ and p-$TO^{14}C$ to the measurement of $TO^{14}C$ after the Ag/Ba/H cartridge pre-treatment.

3.2 Treatment of liquid samples

In the glove box, the outlet valve of the sampling tube was opened, and the alkaline solution was released into a 20 mL vial pre-cleaned with ultrapure water. An aliquot of the liquid sample (ca. 2 mL) was directly used for LSC, gamma (γ) counting (^{60}Co) and TI^{14}C/TO^{14}C analyses (Fig. 2). The remaining portion of the sampled solution (ca. 5 mL) was passed through an Ag/Ba/H cartridge (OnGuard cartridge, Dionex, Sunnyvale, CA, USA) (Fig. 2). This pre-treatment removed interfering anions (e.g. Cl^-) from solution and reduced the pH to ~ 6, which eventually improved peak resolution in ion chromatography (IC). Prior to use, each Ag/Ba/H cartridge was cleaned with 15 mL ultrapure water at a flow rate of 2 mL/min. The first half millilitre of solution collected during pre-treatment was discarded.

3.3 Radio analysis

To determine the ^{60}Co activity, a 1.5 mL aliquot of the sampled solution was transferred into a gamma (γ) vial and diluted with ultrapure water to a total volume of 5 mL. The vial was placed into a Packard Cobra 5003 auto γ-counter (Canberra Packard, Meriden, CT, USA) and the ^{60}Co activity was measured in the energy window between 1'050 and 1'400 keV. Standards were prepared to determine the efficiency of the γ-counter. To this end, different volumes of a ^{60}Co solution (Eckert & Ziegler Isotope Products, Santa Clarita, CA, USA) were diluted in 5 mL ACW. The background was determined (~ 22 cpm) by measuring vials containing ultrapure water or ACW, respectively.

The ^{14}C activity was analysed by LSC in addition to ^{60}Co by γ-counting. The 5 mL solutions previously used for γ-counting were transferred into beta (β) vials and mixed with a 15 mL scintillator (Ultima Gold XR, Packard BioScience, Meriden, CT, USA). The vials were placed in a Canberra Packard Tricarb 2250 CA LSC and the ^{14}C activity was measured in the energy window between 4 and 65 keV. ^{14}C standards were analysed to determine the efficiency of the LSC. For this purpose, different volumes of a ^{14}C-labelled acetate tracer solution (PerkinElmer, Waltham, MA, USA) were diluted in 5 mL acidified ACW. The background (~ 15 cpm) was determined by measuring vials containing ultrapure water or ACW, respectively. A conversion factor for the contribution of ^{60}Co to the β spectrum of ^{14}C was established on the basis of ^{60}Co standard measurements by LSC.

3.4 Non-purgeable organic carbon content

2.5 mL of the cartridge-treated solution were used to determine the concentration of non-purgeable organic carbon (NPOC) by ultraviolet-promoted persulphate wet oxidation and infrared detection of CO_2 (Glaus & Van Loon 2004). The samples were acidified with 20 % H_3PO_4, diluted with ultrapure water to be in the dynamic range of the method (between 1 mg/L and 30 mg/L, detection limit ~ 0.5 mg C/L) and analysed by a Shimadzu TOC-WP® analyser, along with six standard solutions.

3.5 Identification and quantification of dissolved stable carbon compounds

The individual organic compounds were identified and quantified by high performance ion exchange chromatography (HPIEC) using an ICS-5000 IC system (Dionex, Sunnyvale, CA, USA) coupled to an MSQ™ Plus mass spectrometer (MS) (Thermo Fisher Scientific, Waltham, MA, USA). The Chromeleon 6.80 (SR 11d) and the Xcalibur Finnigan Surveyor MSQ 1.1 ELMO software controlled the IC system and MS detector, respectively.

The IC is composed of an AS 50 auto sampler, a 250 mm × 2 mm i.d. IonPac AS11-HC column combined with the corresponding guard column, an EG 40 eluent generator, a 2 mm ADRS–600 suppressor operated in the external water mode and a CD 25 thermal conductivity detector (TCD). The analytical column (thermostat TCC-100, Dionex/Thermo Fisher, USA) was operated at 30 °C using high purity N_2 (grade 6.5, Messer Schweiz AG, Lenzburg, Switzerland) as a protecting and nebulising gas. Pressure was maintained at 5.5 bar.

A volume of 235 µL solution, sampled from the reactor and subjected to pre-treatment with the Ag/Ba/H cartridge (Fig. 2), was spiked with 15 µL of an internal standard containing [d]formic acid and [2,2,2-d_3]acetic acid at 30 µM, [1,3-$^{13}C_2$]malonic acid, [$^{13}C_2$]oxalic acid dehydrate and [d_9]valeric acid at 15 µM (all labelled compounds with a purity grade > 99.5 %; all provided by Sigma-Aldrich, Buchs, Switzerland). The solution was injected into the HPIEC via a 14 µL injection loop and eluted at a flow rate of 0.25 mL/min using KOH as mobile phase. KOH was produced by the eluent generator at 1.0 mM between 0 and 15 min, from 1 to 30 mM between 15 and 35 min, at 30 mM between 35 and 40 min, from 30 to 1 mM between 40 and 41 min, and finally at 1.0 mM between 41 and 50 min.

The MS system is equipped with an atmospheric pressure ionisation (API) interface and operated in the negative electrospray ionisation (ESI) mode with a probe temperature of 500 °C. The ESI needle voltage is -2.5 kV and the cone voltages vary from 30 to 50 V. Optimised MS detection was achieved with a RF lens voltage of -1.0 V, a mass span of 0.5 u and a dwell-time of 0.25 s. Full scan mass spectra were recorded in the range between 20 – 300 m/z at a scan time of 0.5 s. The selected ion monitoring (SIM) mode was used to record the peak intensities (counts/min) of the compounds of interest at their specific m/z values and retention times. The concentration of the analytes was calculated from the area of their respective peaks.

The dynamic range of the analytical method and reproducibility of the IC-MS measurements was checked by using a multi-component stock solution containing sodium formate, sodium acetate (puriss. p.a.), glycolic acid (99 %, Sigma-Aldrich, Buchs, Switzerland), malonic acid (reagent grade 99.5 %, Alfa Aeser, Karlsruhe, Germany), oxalic acid (anhydrous for synthesis, Merck Schuchardt OHG, Hohenbrunn, Germany), sodium l-lactate (> 98 %, Alfa Aeser, Karlsruhe, Germany), valeric acid (> 99 % Sigma-Aldrich, Buchs, Switzerland) and propionic acid Na-salt (> 99 %, Merck Schuchardt OHG, Hohenbrunn, Germany). A total of seven calibration solutions were prepared from the multi-component stock solution in the concentration ranges from 0 to 150 µM (for acetic acid and formic acid) and from 0 to 30 µM (for malonic acid, oxalic acid, glycolic acid, sodium l-lactate, valeric acid and propionic Na-salt). These solutions also contained five isotopic labelled internal standards like [d]formic acid, [2,2,2-d_3]acetic acid, [1,3-$^{13}C_2$]malonic acid, [$^{13}C_2$]oxalic acid and [d_9]valeric acid (purity grade for all labelled compounds > 99.5 %; all provided by Sigma-Aldrich, Buchs, Switzerland) at concentrations 30, 30, 15, 15 and 15 µM, respectively. The limit of detection (LOD) and the limit of quantification (LOQ) of the IC-MS analyses were estimated from the measurements of five blank replicates realised in ACW, according to the procedure of Barwick & Prichard (2011) and Keith et al. (1983) (Tab. 1).

Tab. 1: LOD and LOQ of carboxylic acids analysed by IC-MS

FA = formic acid, AA = acetic acid, OA = oxalic acid, MA = malonic acid, GA = glycolic acid, LA = lactic acid.

	FA	**AA**	**OA**	**MA**	**GA**	**LA**
Retention time [min]	11.6	9.8	31.8	29.8	9.3	8.9
LOD [µM]	3	3	0.05	0.05	0.2	0.2
LOQ [µM]	5	5	0.1	0.15	0.5	0.5

3.6 Total inorganic and organic ^{14}C contents by AMS

The measurements of $TI^{14}C$ and $TO^{14}C$ in untreated solution (d-$TO^{14}C$) were carried out by using EXETAINER® vials (12 mL, screw cap, item 938W, Labco Limited, Lampeter, UK). Prior to use, the vials were immersed overnight in 1 M H_3PO_4, rinsed with ultrapure water, and heated at 500 °C for 5 h to remove any organic contamination. Afterwards, the vials were pressurised at ~ 3 bar with N_2 (using a 25G 5/8" needle) and placed overnight on a hot plate at 75 °C. The vials were considered as gas-tight and further used for sample preparation if a pressure release was ascertained after opening them in the glove box.

The samples were prepared by pipetting 3 × 1.25 mL of the alkaline sample solution into three different vials for triplicate measurements. The solution was spiked with aliquots of ^{14}C-free $KH^{12/13}CO_3$ and $^{12/13}C$-acetate solutions to provide 50 µg of stable carbon that are recommended for reproducible $TI^{14}C/TO^{14}C$ analysis by AMS (LARA, University of Berne). In addition to the samples, three blanks were prepared by adding 1.25 mL ACW to vials containing aliquots of ^{14}C-free $KH^{12/13}CO_3$ and $^{12/13}C$-acetate solutions. The six vials were tightly closed and stored outside the glovebox at -18 °C.

The $TI^{14}C$ and d-$TO^{14}C$ analyses were carried out at LARA (University of Berne). The protocol used for the measurements was reported previously by Rauber (2018). Briefly, the samples were first treated by bubbling He through the alkaline solutions. Then, 0.5 ml 8.5 % H_3PO_4 prepared from 85 % optimum grade H_3PO_4 was injected to acidify the solutions and convert TIC (HCO_3^-, CO_3^{2-}) into CO_2. An auto sampler with a double gas needle consisting of a small inner needle and an outer one was used for CO_2 sampling. Through the inner needle, the solution was purged with He at a flow rate of 50 mL/min. CO_2 was transferred to the gas interface system (GIS) through an opening located in the upper outer needle and injected into the AMS. After the $TI^{14}C$ measurements, 1 mL of oxidising agent (10 % $K_2S_2O_8$ solution in 5 % H_3PO_4 oxidised 1 h before injection to remove carbonaceous impurities) was injected into the vials. Within the two hours of reaction, dissolved TOC was converted into CO_2, which was transferred via the double needle system into the GIS and eventually the AMS for $TO^{14}C$ measurements (d-$TO^{14}C$).

3.7 Sample preparation for measurements of ^{14}C concentrations in solution

3.7.1 $TO^{14}C$

In addition to direct measurement of $TO^{14}C$ (d-$TO^{14}C$), the $TO^{14}C$ was also determined after a cartridge treatment of the solution (p-$TO^{14}C$). To this end, an 800 µL aliquot of the solution, previously filtrated through the Ag/Ba/H cartridge, was spiked with an appropriate aliquot of a 1.25 M ^{14}C-free acetate solution to provide the recommended amount of 20 µg stable carbon. The aliquot was injected into the AMS via an elemental analyser (EA). Details of this analytical method are reported by Cvetković et al. (2018c) and summarised later in Section 3.9.1.

3.7.2 Single aqueous ^{14}C-bearing carbon compounds

An 800 µL aliquot of the solution obtained after cartridge treatment was also pipetted into a pre-cleaned IC vial and spiked with 2 µL of a 6 mM ^{14}C-free acetate solution. The sample was injected successively nine times into the IC and eluted according to the analytical protocol described in Section 3.5. Nine fractions of a single carbon compound of interest (total volume of ~ 500 µL) were successively collected using a fraction collector (Foxy Jr.® Fraction collector, Teledyne ISCO, Lincoln, NE, USA) connected to the outlet of the TCD. AA, FA, LA, MA and OA were the analytes of interest considered for this study. They were collected based on their retention times, which were determined by injecting standards prior to fraction collection.

The ^{14}C concentration of each fraction containing one single ^{14}C-carrying compound was quantified by AMS using two different methods. The first one is based on the oxidative treatment of the organic carbon compounds as previously described for the determination of d-$TO^{14}C$ (see Section 3.6). It was developed at a later stage of the project and therefore not used from the beginning of the corrosion experiment with irradiated steel. The second method was developed in the early phase of the project and consisted of a pre-concentration step. The latter method is described in the following section.

3.7.3 Pre-concentration by freeze-drying

A pre-concentration step based on a freeze-drying procedure was developed with the aim of quantifying ^{14}C concentrations of the single carbon compounds above the LOD of the AMS. To this end, 1 µL 0.1 M NaOH was added to adjust the pH to ~ 11 in the nine separate fractions of AA, FA, LA, MA, and OA collected by IC fractionation (see Section 3.7.2). This step is essential, as the loss of carboxylic acids by evaporation was found to be negligible in alkaline conditions. The samples were weighed, frozen in liquid nitrogen and transferred into a freeze dryer (Alpha 1-2 LDplus, Martin Christ Gefriertrocknungsanlagen GmbH, Osterode am Harz, Germany). It should be noted that only samples containing the same carboxylic acid were freeze-dried together to avoid cross contamination. After approximately three hours of freeze-drying, the nine fractions of each compound were combined to three samples and subjected to an additional freeze-drying step. Then, the triplicates were unfrozen and weighed to determine the pre-concentration factor. The final volume of each sample was ~ 50 µL. Finally, 1 µL 0.1 M HCl and 20 µg ^{14}C-free acetate carrier were added to the samples to re-adjust the pH to ~ 5 – 6 and provide the required amount of stable carbon for reliable ^{14}C AMS measurements. Ultrapure water was treated in the same way (freeze-dried and addition of 20 µg of stable carbon carrier) to check for cross contamination occurring during the freeze-drying process. These samples were used as blanks.

3.8 Analysis of hydrocarbons and sample preparation for AMS

3.8.1 Identification and quantification of gaseous carbon compounds by GC-MS

A TRACE™ GC Ultra gas chromatograph (Thermo Fisher Scientific, Waltham, MA, USA) equipped with an ISQ MS (Thermo Fisher Scientific, Waltham, MA, USA) in the electron ionisation (EI) mode was used to identify and quantify the gaseous carbon compounds. Thermo Xcalibur 3.0.63 (Thermo Fisher Scientific, Waltham, MA, USA) and the PAL Sample Control (PAL3 System software, CTC Analytics AG, Zwingen, Switzerland) were the software controlling the system as well as used for data acquisition and processing.

Before injection into the GC, a 10 mL volume of the sample was withdrawn with a gas-tight syringe (Hamilton AG, Bonaduz, Switzerland) from the gas sampling tube and injected into a purged and evacuated 20 mL headspace vial. For pressure compensation, the headspace GC vial was subsequently connected for 5 seconds to a gasbag filled with N_2. Methane (CH_4; puriss.; 4.5 (GC) from Fluka Analytical, Sigma-Aldrich, Buchs, Switzerland) and a reference gas mixture (Westfalen AG, Münster, Germany) containing 94.8 ppm CH_4 (2.5), 98.3 ppm acetylene (C_2H_2; 2.6), 98.5 ppm ethene (C_2H_4; 2.5), 98.0 ppm ethane (C_2H_6; 2.0), 96.2 ppm propene (C_3H_6; 2.5), 94.1 ppm propane (C_3H_8; 2.5) and 101.0 ppm *n*-butane (C_4H_{10}; 2.5) were used as standard gases to determine the dynamic range of the method and check the reproducibility of the measurements. For this purpose, between 0.3 and 10 mL volume of the standards were withdrawn from the gas bag, diluted with N_2 if necessary in a Hamilton syringe and injected into headspace GC vials. Five blank replicates consisting of five headspace GC vials filled with N_2 were additionally analysed to determine the LOD and LOQ of the GC-MS measurements (Tab. 2), in line with Barwick & Prichard (2011) and Keith et al. (1983).

All samples, standard gases and blanks were injected into the GC-MS with the headspace technique using the following procedure. After 120 seconds incubation at 50 °C under agitation, 2 mL of the gas volume of the headspace GC vial were injected into the GC via a gas-tight syringe preheated at 85 °C. The injections were performed in split mode with a ratio of 1:18 using He (Carbagas AG, Muri, Switzerland, grade 5.0) as carrier gas at a constant flow rate of 2.0 mL/min. A Restek Rt®-Msieve 5A column (30 m × 0.32 mm with 0.025 mm film; named column 1) was used in combination with a specific temperature programme to achieve a well-resolved separation of the HCs. The temperature programme was as follows: start at 45 °C (hold 4 min) and increase to 290 °C at a rate of 20 °C/min (hold 10 min). The run time was ~ 26 min. The MS was operated at standard EI parameters with a collision energy of 70 eV, an EM voltage of 1'860 V, and a source temperature of 230 °C. Data were acquired in the SIM mode, as for the IC-MS analysis.

Tab. 2: LOD and LOQ of HCs analysed by GC-MS

	Methane	**Ethane**	**Ethene**	**Propane**	**Propene**	**Butane**
Retention time [min]	2.8	10.5	15.3	15.7	20.4	22
LOD [µM]	0.02	0.005	0.007	0.01	0.005	0.02
LOQ [µM]	0.05	0.017	0.020	0.03	0.017	0.05

3.8.2 Sampling of hydrocarbons in the fraction collector

The quantification of single gaseous ^{14}C-bearing HCs by AMS required the development of a procedure similar to the one previously developed for single dissolved ^{14}C-bearing carbon compounds (see Section 3.7.2). To this end, a new set-up allowing the collection of single HCs was developed by connecting a custom-made fraction collector at the outlet of the non-destructive thermal conductivity detector (TCD) (Fig. 3). The fraction collector consists of a collection valve, seven loops (#2 to #8) and a purge valve controlled by a custom-made software. The collection valve starts and stops the trapping of the analytes of interest in the sampling loops in accordance with their retention time. Loop #1 is only a by-pass. The purge valve is used to flush each loop with He for several minutes before trapping to avoid any contamination with air. The device was developed by Brechbühler AG (Switzerland), the commercial partner in the project.

The GC-TCD system is operated with the Thermo Xcalibur 3.0.63 software (Thermo Fisher Scientific, Waltham, MA, USA) for data acquisition and processing, while a custom-made software from Brechbühler AG (Schlieren, Switzerland) controls the different valves of the fraction collector. Various gases were used during the course of the development and optimisation of the new set-up: He (Carbagas AG, Muri, Switzerland, grade 5.0) as carrier gas, N_2 (Carbagas AG, Muri, Switzerland, grade 5.0) to switch the different valves of the GC, fossil CH_4 (puriss.; 4.5 (GC) from Fluka Analytical, Sigma-Aldrich, Buchs, Switzerland), modern CH_4 (GPC Radiocarbon lab, University of Berne; $F^{14}C = 1.024 \pm 0.003$; see Espic et al. 2019), C_2H_6 (Carbagas AG, Muri, Switzerland, grade 5.0), C_3H_8 (puriss.; 2.5 (GC) from Westfalen Gas GmbH, Eiken, Switzerland) and C_4H_{10} (puriss.; 2.5 (GC) from Westfalen Gas GmbH, Eiken, Switzerland) as standard gases.

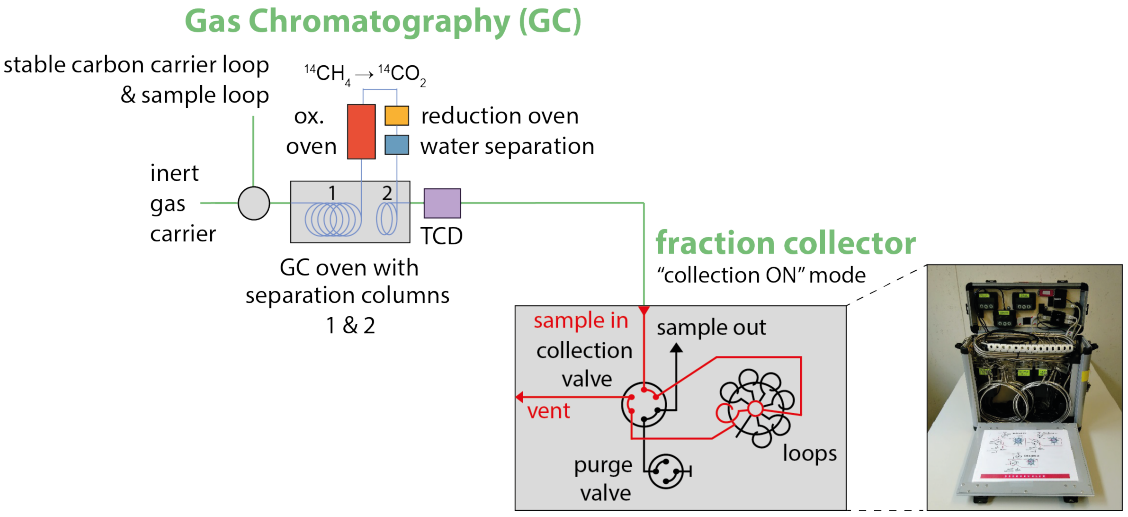

Fig. 3: Analytical set-up for separation and collection of gaseous carbon compounds by coupling a GC-TCD to a fraction collector

A picture of the fraction collector is shown on the right.

Injections of the gas samples and carriers were carried out as follows. The gas sample containing the analyte of interest was loaded into an injection loop (called sample loop) having a volume of 500 µL. At the same time, a stable ^{14}C-free carbon carrier (for instance CH_4 or C_2H_6) was loaded into a second loop (named carrier loop) with a volume of 40 µL, corresponding to a capacity of 20 µg C at ambient pressure, which is the amount of stable carbon ($^{12/13}C$) recommended for reproducible ^{14}C AMS measurements. The two loops were simultaneously injected into the GC in split mode, as described in the previous Section 3.8.1. After injection, the HCs were separated with the Restek Rt®-Msieve PTL-5A column (30 m × 0.32 mm with 0.025 mm film; named column 1) (Fig. 3) in combination with a specific temperature programme. It starts at an initial temperature of 50 °C (hold 4 min) and is followed by a first heat up to 80 °C at a rate of 20 °C/min and by a second one at a rate of 50 °C/min to the maximum temperature of 290 °C (hold 10 min). The single HCs separated by the chromatographic Restek column were oxidised to CO_2 in the oxidation oven (Thermo Fisher Scientific, Bremen, Germany) (Fig. 3). The oxidation oven is a non-porous alumina tube (Al_2O_3; 0.5 mm i.d.; 1.55 mm o.d.), in which three wires of copper (Cu), nickel (Ni) and platinum (Pt) of identical length (240 mm) and diameter (0.125 mm) are braided and centred end-to-end. The Cu/Ni/Pt catalyst is inserted into the resistively heated Al_2O_3 furnace (1.6 mm i.d.; 260 mm length; 32 Q cold resistance) and its normal operating temperature is 1'000 °C. Then, the oxidation products (i.e. mainly CO_2) pass through a reduction oven to remove traces of O_2 and nitrous oxides (NO_x). The oven consists of three wires of Cu (0.125 mm diameter) (Fig. 3) and it is operated at 650 °C. Residual water is removed from the analyte stream by a water separator connected after the reduction oven (Fig. 3). It is composed of a glass tube (4 mm i.d.; 6 mm o.d.) with a NAFION™ membrane (Permature, Toms River, NJ, USA; 0.3 mm i.d.; 0.6 mm o.d.; 20 cm length) continuously purged by a counter-current stream of dry He at a flow rate of 3 – 4 mL/min. The analyte stream, free of O_2, NO_x and water, further passes through a short, second separation column (Restek Rt®-Msieve PTL-5A column; 0.5 m × 0.32 mm with 0.025 mm film; named column 2) which allows CO_2 to be separated from non-oxidised HCs (e.g. CH_4). Both CO_2 and non-oxidised carbon compounds are finally detected by the non-destructive TCD (Thermo Finnigan GC-combustion interface III). Eventually, the compounds of interests were collected in the seven trapping loops of the fraction collector in the chemical form of CO_2 based on their retention time (Fig. 3). The total run time of the procedure was ~ 20 min per sample.

In this study, we also intended to determine the total ^{14}C content of the gas phase ($TG^{14}C$). To this end, column 1 was replaced by a fused Si capillary (1 m × 0.32 mm) and the temperature programme of the GC oven was adjusted: it started at 150 °C (hold 4 min) and heated up to 290 °C (hold 5 min) at a rate of 40 °C/min. With this set-up, trapping of all ^{14}C-bearing carbon compounds present in the gas phase by the fraction collector was achieved. The run time per sample was only 12.5 min.

3.9 ^{14}C detection by AMS

3.9.1 ^{14}C quantification in liquid samples by AMS

^{14}C quantification of the single dissolved carbon compounds (acetic acid, formic acid, lactic acid, malonic acid, oxalic acid) and $p\text{-}TO^{14}C$ were conducted at LARA (University of Berne), using an online injection set-up previously described in Ruff et al. (2010a,b) and Salazar et al. (2015). It consists of an EA (Vario Micro Cube, Elementar Analysensysteme GmbH, Langenselbold, Germany) coupled to the MICADAS via the GIS and involves the separation of the high load of He (the carrier gas) from the microgram level of CO_2 (stable carbon and ^{14}C-labelled) during its release into the GIS and subsequent slow injection into the MICADAS. In brief, 10 µL of the liquid samples or standards were tightly packed in tin capsules for flash combustion, loaded by an auto-sampler into the oxidation oven of the EA and combusted with a pulse of O_2 at 850 °C. The carrier gas (He) transfers the gases resulting from the sample combustion through a water

trap containing SICAPENT® (Merck KGaA, Darmstadt, Germany) onto a zeolite trap, which is heated up stepwise to consecutively release N_2, CO_2 and the residual gases. Only the CO_2/He mixture is directed into a second zeolite-based CO_2 trap inside the GIS (zeolite X13, Sigma-Aldrich, Steinheim, Germany) through a 1/16" o.d. tubing (10 m long) at a flow rate of 80 mL/min. After CO_2 collection, the zeolite trap is heated up to 450 °C and CO_2 is released into a syringe of known volume, whose plunger is controlled by a stepper motor (Fig. 4). Eventually, a final gas mixture of 10 % CO_2 at ~ 0.16 MPa is made by adding He to the syringe, which is transferred into the MICADAS ion source at a flow rate of ~ 40 µL/min (Fig. 4). During the ^{14}C measurements in the MICADAS, the EA-GIS system is flushed for 4 min. This procedure consists of running a blank combustion in the EA at 100 mL/min and heating up gradually the CO_2 trap of the EA. The flow is then directed to the GIS trap, which, at the same time, is heated up for flushing. The procedure is automated and controlled by a LabView programme reported by Wacker et al. (2013).

3.9.2 ^{14}C quantification in gaseous samples by AMS

Once the HCs were trapped as CO_2 in the loops of the fraction collector (see Section 3.8.2), the fraction collector was disconnected from the GC system and transferred to LARA, where it was connected to the GIS through a 1 m long 1/16" o.d. tubing (Fig. 5). A He flow rate of typically ~ 30 mL/min was applied during 150 – 300 s to flush CO_2 from the sampling loops of the fraction collector onto the GIS zeolite trap (Wacker et al. 2013, Salazar et al. 2015). The flush/load time was applied in accordance with the volumes of the sampling loops and the flow rate determined after each loop. Hence, the trapping time was increased with decreasing flow rate. Eventually, CO_2 was released from the zeolite trap of the GIS and injected into the AMS, as previously described in Section 3.9.1.

3.9.3 Operation of the MICADAS

The MICADAS system used for the ^{14}C quantification at LARA is comparable to large AMS systems in terms of accuracy, precision, and detection limit. It offers advantages due to the simplified instrumental set-up that reduces running costs and service efforts. Its operation is user-friendly and ^{14}C analyses require low amounts of sample material and allow a short process time (Szidat et al. 2014). In the MICADAS, samples are ionised and the rare ^{14}C isotope is directly detected along with the abundant ones (i.e. ^{12}C and ^{13}C) (Fig. 6). The results are expressed in terms of $^{14}C/^{12}C$ ratios. The removal of isobaric interferences (interferences from equal mass isotopes of different elements exemplified by ^{14}N in ^{14}C analysis), isotopic interferences (interferences from equal mass to charge isotopes of different elements), and molecular interferences (interferences from equal mass to charge molecules, such as $^{12}CH_2^-$, ^{12}CD or $^{13}CH^-$ in ^{14}C analyses) is the main challenge during ^{14}C AMS measurements.

After CO_2 release from the zeolite trap of the GIS and injection into the gas ion source, a primary beam of thermally ionised Cs vapour (Cs^+) is sputtered on the sample target (i.e. CO_2) at 130 °C and 128 W. Only the negatively charged ions (i.e. $^{12}C^-$, $^{13}C^-$ and $^{14}C^-$) are extracted and fed into the accelerator (Fig. 6). There, high-energy collisions and charge exchange with a "stripper tube" material, containing a gas, rip off electrons from the particles, destroying the integrity of most molecular interferences (isobars: ^{13}CH, $^{12}CH_2$) and change the charge of the ions from negative to positive. The electric field repulses and accelerates the ions further as a result of charge inversion (Synal et al. 2007) (Fig. 6). Eventually, the beam is filtered one more time on the high energy beam line before ion detection and counting by the Faraday cups (for ^{12}C and ^{13}C) and the ionisation chamber (for ^{14}C) is realised (Kutschera 2005) (Fig. 6). MICADAS is controlled and accessed by Transmission Control Protocol/Internet Protocol commands generated by a control programme written in LabView.

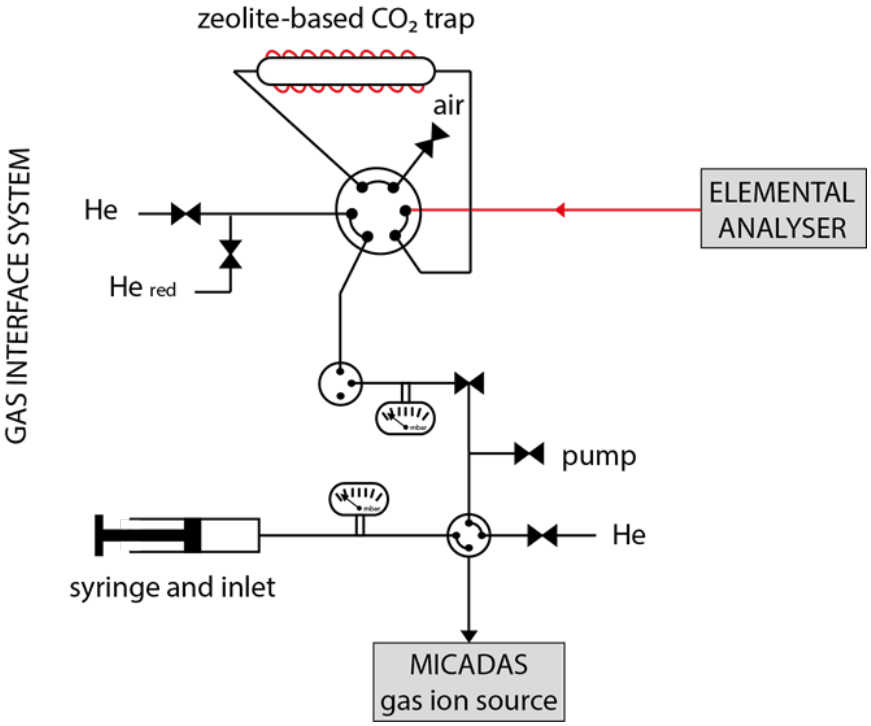

Fig. 4: Connection between the EA and the ion source of the MICADAS via the GIS according to Salazar et al. (2015)

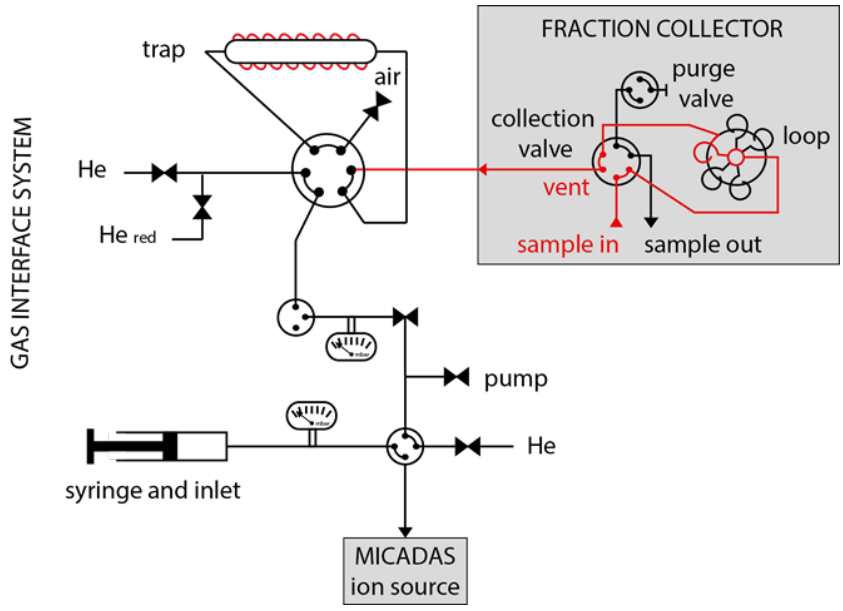

Fig. 5: Connection between the fraction collector and the ion source of the MICADAS via the GIS according to Salazar et al. (2015)

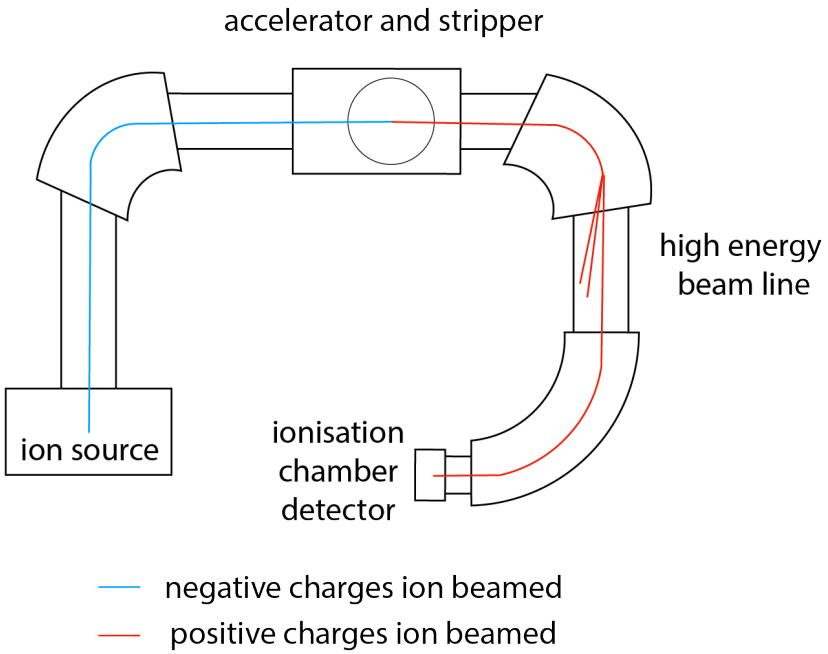

Fig. 6: Schematic layout of a MICADAS according to Rauber (2018) and Synal et al. (2007)

The standards used to calibrate the MICADAS were 5 % CO_2 from oxalic acid II (National Institute of Standards and Technology; SRM 4990C) in He prepared by Hekal AMS C-14 laboratory (Debrecen, Hungary) with $^{14}C/^{12}C$ of 1.3407 ± 0.0005 and 4.5 % fossil CO_2 in He (Messer AG, Lenzburg, Switzerland).

4 Results and discussion

4.1 Quantification of dissolved ^{14}C-bearing carbon compounds

4.1.1 Recovery of dissolved organic carbon compounds by HPIEC

The separation of dissolved organic carbon compounds by HPIEC was optimised for FA, AA, LA, OA, and MA, which were expected to be the main oxidised carbon compounds produced during alkaline anoxic corrosion of irradiated steel (Cvetković et al. 2018b). A mixture containing AA, FA, and LA at 500 µM as well as OA and MA at 200 µM was injected into the IC to determine the recovery rate and to test repeatability of the HPIEC measurements. After IC fractionation, the concentrations of the single carboxylic acids were quantified by TCD. The recovery rate was determined by comparing the concentrations of the compounds (in triplicates) before and after IC fractionation. The rates were equal to 95 ± 6 % for FA, 100 ± 7 % for AA, 99 ± 3 % for MA, 96 ± 4 % for OA and 98 ± 2 % for LA. Thus, complete recovery and excellent repeatability of the IC fractionation process were observed.

4.1.2 ^{14}C background

The scoping calculations showed that ultra-low ^{14}C concentrations (in femto to pico molar) will be released into solution and gas phase during the alkaline anoxic corrosion of irradiated steel. Therefore, any contamination with ^{14}C has to be avoided. To achieve this, special care was taken to minimise contamination by the vials, "natural" atmospheric ^{14}C (i.e. $^{14}CO_2$), water, leaching solutions and sample treatments.

The ^{14}C background of different types of sample vials was determined by AMS using a ^{14}C-free sodium acetate solution (2 µg stable carbon/µL) as carrier. The vials were immersed in ultrapure water in a closed container for a period of at least 7 days, while the water was replaced daily (Cvetković et al. 2018c). The effect of this cleaning procedure on the background was tested for different types of vials and two different waters (Cvetković et al. 2018c). No significant difference in the ^{14}C background for pre-cleaned plastic and glass vials was observed (Tab. 3). Furthermore, the water having a LC-MS grade quality (CHROMASOLV^{TM}, LC-MS ultra, Merck KGaA, Darmstadt, Germany) showed a similar background as compared to degassed ultrapure water (between 13 and 11 ± 4 fM) (Tab. 3) (Cvetković et al. 2018c). By contrast, a significant increase in the ^{14}C concentration was observed for ACW, which was not pre-treated by an OnGuard® cartridge (123 ± 67 fM; 0.63 ± 0.34 $F^{14}C$). This increase in the ^{14}C background is most likely caused by the ingress of atmospheric CO_2 (containing a contemporary concentration of $^{14}CO_2$) into the alkaline solution during sample preparation, transportation and AMS measurement (Cvetković et al. 2018c). Thus, it was concluded that alkaline solutions should either be handled under a controlled $^{14}CO_2$-free atmosphere (glovebox) or neutralised immediately after sampling to avoid the ingress of atmospheric $^{14}CO_2$.

The ^{14}C background of the different sample treatments, such as pre-treatment using the OnGuard® cartridge and IC fractionation, was determined by using ultrapure water and ACW. The samples were filtrated through the OnGuard® cartridge, injected into the IC, collected at the same retention time of the targeted carbon compounds, and analysed by AMS. A similar background was observed when injecting either degassed ultrapure water or ACW into the IC system and collecting the eluent at the retention times of the different carboxylic acids (Tab. 3) (Cvetković et al. 2018c). Various materials (e.g. analytical column, eluent, and laboratory atmosphere) could also interact with the sample during fractionation and enhance the ^{14}C background. However, the backgrounds determined after pre-treatment of the solutions with the

OnGuard® cartridges and IC fractionation were comparable to the ones determined for degassed ultrapure water, which was not subjected to IC fractionation (Tab. 3). This finding shows that no enhancement in the ^{14}C background occurred during IC fractionation. In order to avoid additional ^{14}C ingress and microbial degradation of the organic carbon compounds, all samples prepared for AMS measurements were frozen and stored at -20 °C immediately after fractionation.

The LOD can be estimated taking into account the average of the blank measurements (a_{blank}) and the standard deviation of the blank measurements (s_{blank}) according to the equation: $LOD = a_{blank} + 3.3 \cdot s_{blank}$ (Barwick & Prichard 2011). By using the ^{14}C background of pre-cleaned polypropylene vials at 12 ± 4 fM (or 0.06 ± 0.02 $F^{14}C$), the LOD was determined to be equal to 23 fM or 0.12 $F^{14}C$ (Tab. 3).

Tab. 3: ^{14}C background measurements reported by Cvetković et al. (2018c)

1 fM corresponds to 10^{-15} mol/L.

Vial [fM]		**Solvent** [a] [fM]		**IC fraction** [b] [fM]			
poly-propylene	11 ± 4	ultrapure water	11 ± 4	ultrapure water-AA	13 ± 5	ACW-AA	12 ± 4
glass	12 ± 4	LC-MS Ultra water	13 ± 4	ultrapure water-FA	8 ± 7	ACW-FA	10 ± 5
		degassed ultrapure water	21 ± 13	ultrapure water-MA	5 ± 3	ACW-MA	12 ± 5
		ACW (pH 12.5)	123 ± 67	ultrapure water-OA	4 ± 3	ACW-OA	11 ± 3

[a] Tests performed using pre-cleaned polypropylene vials. Ultrapure water refers to deionised, de-carbonated water generated by a Milli-Q gradient A10 purification system (Merck Millipore, Billerica, MA, USA). LC-MS Ultra water had LC-MS grade quality (CHROMASOLV™, LC-MS Ultra, Merck KGaA, Darmstadt, Germany). See Section 3.1 for the preparation of ACW.

[b] Ultrapure (Milli-Q) water was injected into the IC and collected at the retention time of selected target carbon compounds, i.e. AA, FA, MA and OA.

4.1.3 Recovery tests with ^{14}C-bearing carbon compounds

Tests were carried out with the ^{14}C-bearing carboxylic acids (^{14}C-AA, ^{14}C-FA, ^{14}C-MA and ^{14}C-OA) to determine the recovery of these compounds during fractionation and the dynamic range of the AMS. To this end, standards containing ^{14}C-labelled carboxylic acids at different concentrations in ultrapure water were injected into the IC system. The fractions were collected at the specific retention times of the compounds and their ^{14}C content was quantified by AMS (Cvetković et al. 2018c). The recovery rate was calculated from the ratio of the injected concentrations (denoted as "expected") and the measured ones. Only the results obtained with ^{14}C-AA are shown in Tab. 4 as close to 100 % recovery was observed for all compounds.

The expected concentrations of ^{14}C-AA ranged between 39 and 9881 fM and the measured ones between 26 ± 9 and 8'965 ± 456 fM, corresponding to 0.2 – 50.5 $F^{14}C$ in a matrix of 20 µg stable carbon. Note that a 1:50 dilution of the samples occurred during the IC injection/ collection steps. A very good agreement between the expected concentrations and the concentrations determined by AMS after IC fractionation was observed with a mean recovery rate of 93 ± 9 % (Tab. 4).

Nevertheless, a rather poor recovery was found at the lowest concentration (Tab. 4), presumably due to the lower precision of the measurements when the ^{14}C concentrations are close to the LOD (Cvetković et al. 2018c). Thus, these experiments enabled us to determine the linear dynamic range of the AMS measurements between 0.01 pM ^{14}C (0.06 $F^{14}C$) and 14.8 pM ^{14}C (75 $F^{14}C$). However, as undesirable memory effects were observed in the AMS measurements at the highest ^{14}C concentrations, the maximum applicable concentration was limited to 9.8 pM ^{14}C (50 $F^{14}C$). Hence, the linear dynamic range extends over three orders of magnitude (Cvetković et al. 2018c), providing sufficient flexibility for ^{14}C measurements.

Tab. 4: Recovery of ^{14}C-bearing AA after IC fractionation and AMS detection according to Cvetković et al. (2018c)

Expected [$F^{14}C$]	**Expected** [fM]	**Measured** [fM]	**Recovery** [%]
0.21	39	26 ± 9	67 ± 23
0.53	104	103 ± 13	99 ± 12
1.06	207	191 ± 17	92 ± 8
3	586	572 ± 36	98 ± 6
4.95	968	1'011 ± 58	104 ± 6
11.73	2'296	2'220 ± 119	97 ± 5
25.3	4'951	4'562 ± 236	92 ± 5
50.5	9'881	8'965 ± 456	91 ± 5

Additional series of recovery tests were carried out with solutions containing either individual ^{14}C-labelled carboxylic acids (i.e. ^{14}C-FA, ^{14}C-AA, ^{14}C-MA, ^{14}C-LA, ^{14}C-OA) or a mixture of all of them with the aim of quantifying the recovery of the entire sequence of sample preparation steps (i.e. the OnGuard® cartridge pre-treatment and subsequent IC fractionation). For this purpose, standards with an initial concentration of 9.8 pM ^{14}C (50 $F^{14}C$) were prepared in ACW at pH 12.5 and passed through the Ag/Ba/H cartridge, injected into the IC and collected separately at the retention time of the individual carboxylic acids. The recovery rates were estimated by considering the dilution factor during IC fractionation for each compound. A complete recovery was determined for ^{14}C-FA, ^{14}C-AA, ^{14}C-MA and ^{14}C-LA, whereas only 50 % of the initial ^{14}C-OA concentration injected in the Ag/Ba/H cartridge was measured after IC fractionation. Similar tests were previously carried out by Cvetković et al. (2018c). These authors reported similar results except for ^{14}C-MA, which had a recovery of only 50 %. Several repetitions of these tests by using solutions containing a mixture of both stable carbon and ^{14}C-labelled carboxylic acids diluted in ACW at pH 12.5 in the concentration ranges expected in the reactor confirmed full recovery for ^{14}C-MA, in addition to ^{14}C-AA, ^{14}C-FA, and ^{14}C-LA, while reduced recovery was confirmed for ^{14}C-OA (i.e. ~ 50 %). The reason for the discrepancy of the ^{14}C-MA recovery between the two studies is presently not clear. However, the lower recovery of ^{14}C-OA was found to be highly reproducible. Although the reason is still unknown, it indicates retention of OA in the cartridge (e.g. by precipitation or the formation of a solid solution) rather than a loss of ^{14}C-OA during IC fractionation (see Section 4.1.1). In the light of these results, a full recovery was considered for ^{14}C-AA, ^{14}C-FA, ^{14}C-LA, ^{14}C-MA, while the HPIEC and AMS data obtained for stable $^{12/13}C$- and ^{14}C-carrying OA were corrected in accordance with a reduced recovery rate of 47 ± 4 %.

4.1.4 Cross contamination

Cross contamination was considered to be possible during IC fractionation and ^{14}C detection by AMS. The following tests were carried out to address the possibility of cross contamination. They are described in detail in Cvetković et al. (2018c).

IC fractionation: Alternating samples of ^{14}C-depleted and ^{14}C-labelled carboxylic acids with the highest ^{14}C concentration (corresponding to 2'500 $F^{14}C$ in a matrix of 20 µg stable carbon) were injected into the IC. The eluate was collected according to the retention times of the carboxylic acids of interest. Only the ^{14}C-depleted samples were analysed by EA-GIS-AMS. The ^{14}C background was not enhanced after injection of the ^{14}C standards even at the highest concentration, indicating that no cross contamination occurred during IC fractionation (Cvetković et al. 2018c).

IC-EA-AMS measurements: Cross contamination could occur in the EA and GIS, when samples with a wide range of concentrations are analysed. If the concentration (R_x) and mass (m_x) of the previous active samples are high enough, it is possible that a small fraction (φ) remains inside of the measuring instrument, mixing with the mass (m_s) and concentration (R_s) of the next sample. The mixing will therefore lead to an incorrect measured concentration (R_m). As the cross contamination is considered to be constant for the analysis of $^{14}C/^{12}C$, it is therefore possible to subtract and correct the contamination from the measured value. A ^{14}C mass balance analysis of cross contamination was reported by Salazar et al. (2015):

$$R_m - R_s = \frac{\varphi m_x}{m_s}\left(R_x - R_s\right) \tag{3}$$

^{14}C-labelled AA (R_x) and ^{14}C-depleted sodium acetate (R_s = 0 $F^{14}C$) were alternatively injected into the IC. The eluate was collected and analysed with the set-up EA-GIS-AMS, with the alternating order. It should be noted that the sample mass for both substances was kept constant ($m_s = m_x$ = 20 µg). The slope obtained by plotting R_m vs. R_x corresponds to the cross-contamination factor φ = 0.45 % (Fig. 7a). The $^{14}C/^{12}C$ ratios displayed in Fig. 7a were corrected using the following equation:

$$R_{corr} = \left(\frac{m_s R_m - \varphi m_x (R_x - R_0)}{m_s - \varphi m_x}\right) \tag{4}$$

The results are displayed in Fig. 7b. A comparison of the previously determined background level (0.06 ± 0.02 $F^{14}C$) with the corrected ratio (Fig. 7b) reveals that the contaminated values of the ^{14}C-depleted substance returned to the background level (Cvetković et al. 2018c). Thus, these results support the proposed fitting and correction for cross contamination. Cross contamination could affect the measurements at high ^{14}C concentrations and should therefore be taken into account in the data treatment of all samples (Cvetković et al. 2018c).

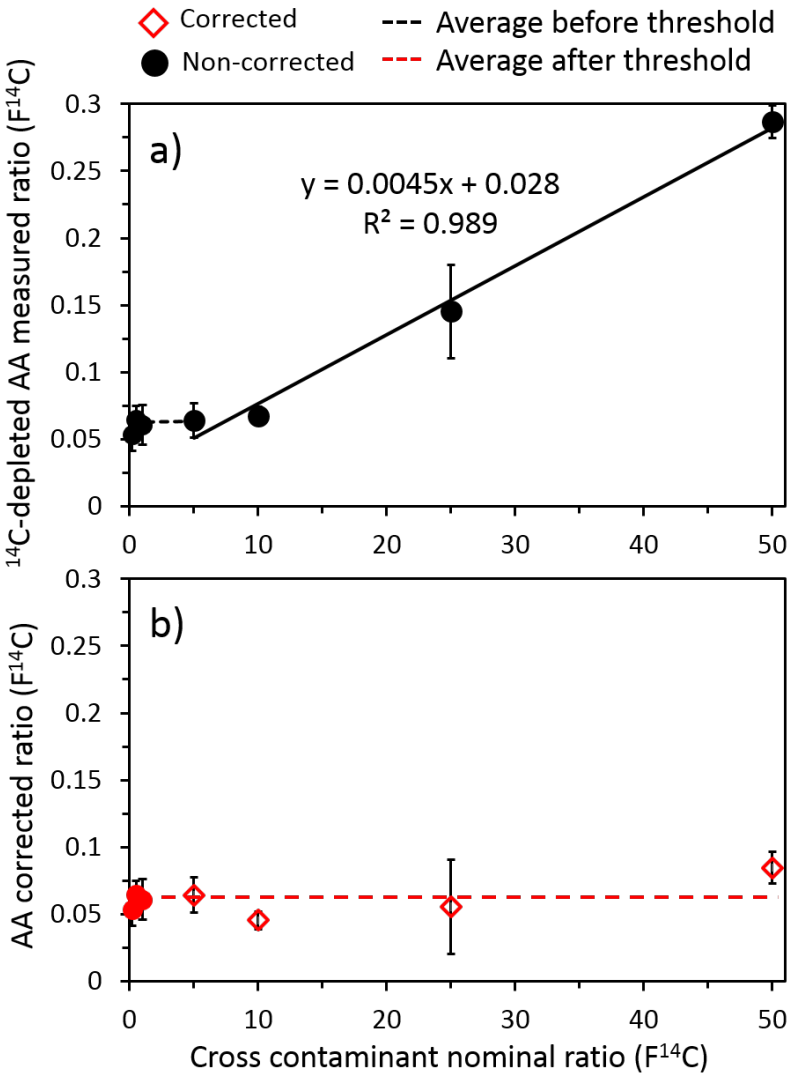

Fig. 7: Characterisation of the cross contamination for the entire IC-EA-GIS-AMS system according to Cvetković et al. (2018c)

Samples were injected into the IC and analysed with the EA-GIS-AMS system. a) Measured F^{14}C of AA depleted in ^{14}C, which was cross contaminated with a previous injection of AA having a high ^{14}C/^{12}C ratio ("hot sample"). The closed circles indicate the region where the cross contamination model behaves linearly. b) Same data as (a) but the cross contamination was linearly corrected using Eq. 4 for "hot samples". R_x values are equal or higher than the threshold (R_0 = 5 F^{14}C). The closed circles indicate the start of the region where cross contamination is small, extending until the beginning of the linear region indicated by the dashed line.

4.2 Quantification of gaseous ^{14}C-bearing carbon compounds

4.2.1 Requirements for CSRA

Previous batch-type experiments carried out with iron powders immersed in alkaline ACW solution showed a release of small HCs (up to C7) in the gas phase (Cvetković et al. 2018a, Guillemot et al. 2020). Furthermore, CH_4 was found to be the dominant HC formed during iron corrosion. The development of CSRA for the ^{14}C-bearing HCs formed during the corrosion of irradiated steel was based on the assumption that similar carbon compounds could be formed during corrosion of iron powders and irradiated steel. It was therefore expected that CH_4 will be one of the main HC present in the gas phase during the alkaline anoxic corrosion of irradiated steel. As a consequence of the above assumption, CH_4 was used as standard during the development and optimisation of the CSRA for ^{14}C-bearing HCs.

A recommended amount of 20 µg ^{12}C is required in each sample subjected to AMS for obtaining reproducible ^{14}C measurements at LARA. To this end, ^{14}C-free gas carrier was added, such as fossil CH_4, via injection carrier loops having capacities between 20 and 60 µg of stable carbon. The loops allow the amount of carrier required for ^{14}C AMS measurements to be injected into the GC-TCD simultaneously with the sample. Note that the amount of carrier added was optimised at a later stage of the project.

The following sections document the stepwise approach for developing and optimising CSRA for ^{14}C-carrying HCs. The development and optimisation aimed at: (i) determining the recovery rate of the HCs during their fractionation by GC, (ii) collection by the custom-made fraction collector and injection into the AMS, and (iii) obtaining reproducible ^{14}C AMS measurements. The following recovery tests were essential as a loss of stable carbon (and sample) could occur in all stages of sample preparation, e.g. in the GC-TCD set-up, the fraction collector, during the CO_2 release from the fraction collector loops into the GIS and/or during CO_2 release from the GIS into the MICADAS (Figs. 3 – 5).

4.2.2 Carbon recovery in the GC-TCD system

4.2.2.1 Test of the injection mode

The test of the injection mode was carried out by loading the carrier loop (60 µL) with 30 µg C in the chemical form of fossil CH_4 and the sample loop with 500 µL N_2. N_2 was chosen to be injected via the sample loop during the CSRA development because it is already present in the reactor to maintain anoxic conditions. The loadings from the two loops were simultaneously injected by the GC injector in split mode at a splitless time of 1 min. During this time, the split line is closed and the CH_4/N_2 mixture, stored in the glass liner, reaches the GC column (Fig. 8). However, as soon as the splitless time (1 min) is over, the remaining gas present in the liner is flushed out through the split line into the vent and therefore not subjected to analysis (Fig. 8).

The splitless injection time was varied with the aim of testing its effect on the recovery of stable carbon (Fig. 9). When the splitless time was set at 2 min, the full shapes of the N_2 peak (injected via the sample loop) and the one of CO_2 (corresponding to CH_4 injected via the carrier loop and oxidised to CO_2 in the oxidation oven) were recorded (Fig. 9). This indicates that complete recovery occurred at a splitless time of 2 min and the total amount of injected gas reached the GC column. Nevertheless, Fig. 9 clearly shows that the retention time of the two elution peaks (i.e. N_2 and CO_2) were very close to each other, meaning that co-elution of carbon compounds could occur, and their peaks might overlap. In case of an overlap of the peaks, the individual compounds

cannot be collected separately by the fraction collector, which is not desired for the CSRA of the ^{14}C-bearing HCs. Consequently, we decided to retain a splitless injection time of 1 min, knowing that a portion of the injected gas is lost via the vent. This loss was quantified by comparing the areas of the two CO_2 peaks recorded by the TCD at the splitless injection times of 2 and 1 min (Fig. 9). The peak areas were determined to be 1.62×10^7 a.u. for the splitless time of 2 min and 1.29×10^7 a.u. for the splitless time of 1 min. The recovery rate was assumed to be 100 % at the splitless time of 2 min, which resulted in 80 % recovery at a splitless time of 1 min.

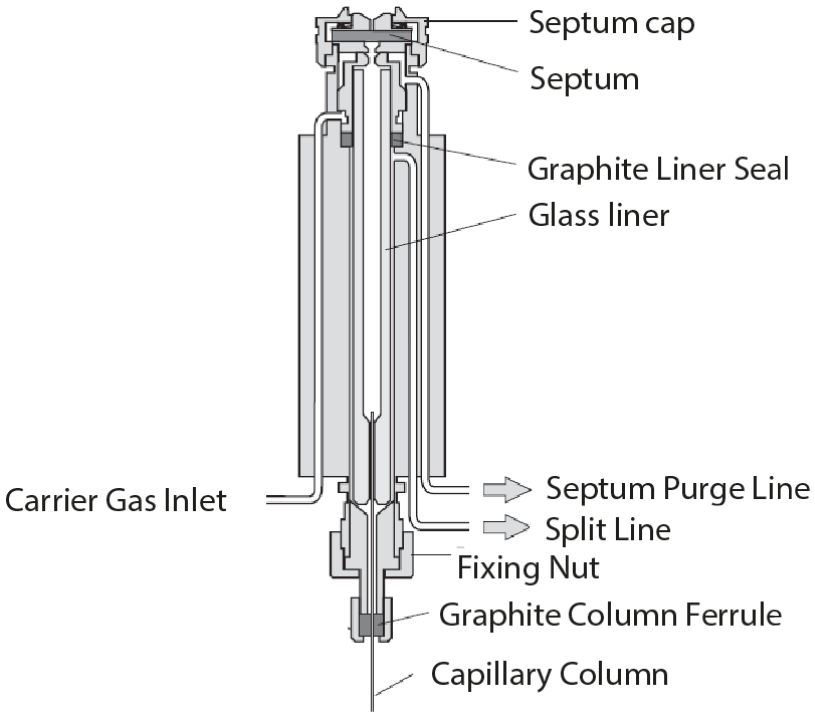

Fig. 8: Representation of a split/splitless injector according to Thermo Fisher Scientific (2010)

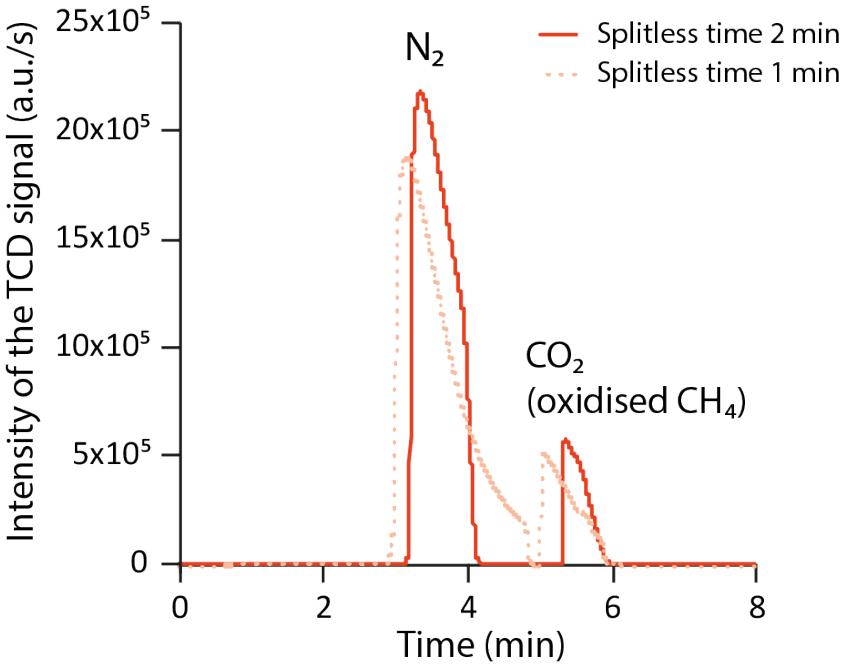

Fig. 9: N_2 and CO_2 peak shapes and areas obtained with a splitless injection time of 2 min (dark red solid line; CO_2 peak area recorded by TCD = 1.62×10^7 a.u.) and with a splitless injection time of 1 min (light red dotted line; CO_2 peak area registered by TCD = 1.29×10^7 a.u.)

The peak shapes and areas of N_2 and CO_2 cannot be directly compared due to differences in the concentrations injected and the TCD sensitivity for these two molecules.

4.2.2.2 Test of efficiency and capacity of the oxidation oven

The individual carbon compounds were separated from each other by passing through the GC column 1. Then, they reached the catalyst (three Cu/Ni/Pt wires) of the oxidation oven in which they were converted into CO_2. Injections of CH_4 were realised with the oxidation oven switched off (T = 400 °C) and on (T = 1'000 °C) to test the efficiency of the oxidation process. With the oxidation oven switched off, N_2 and CH_4 were detected by the TCD at almost the same retention time, i.e. N_2 between 3 and 3.5 min and CH_4 between 3.5 and 4.5 min, and co-eluted (Fig. 10). Note that it was only possible to distinguish between N_2 and CH_4 because the amount of injected N_2 was lower than 500 µL N_2 in this case (Fig. 10). The N_2 peak would completely cover the one of 30 µg C (injected as CH_4 via the 60 µL loop) by injecting 500 µL N_2 instead of the 50 µL N_2 used in this case. Thus, co-elution of N_2 and CH_4 did not allow us to verify if CH_4 was converted to CO_2 with the oxidation oven switched on. As a consequence, He, which is not detected by the TCD, was injected via the sample loop instead of N_2 (Fig. 10). This resulted in one major peak recorded by the TCD at a retention time between 5.0 and 5.7 min, corresponding to CO_2 (i.e. CH_4 converted to CO_2 in the oxidation oven). No other peak was detected between 3.5 and 4.5 min, which corresponds to the retention time of the non-oxidised CH_4 (Fig. 10). This finding shows that the total amount of C injected as fossil CH_4 (30 µg C via 60 µL loop) was completely oxidised to CO_2 indicating 100 % efficiency of the oxidation oven.

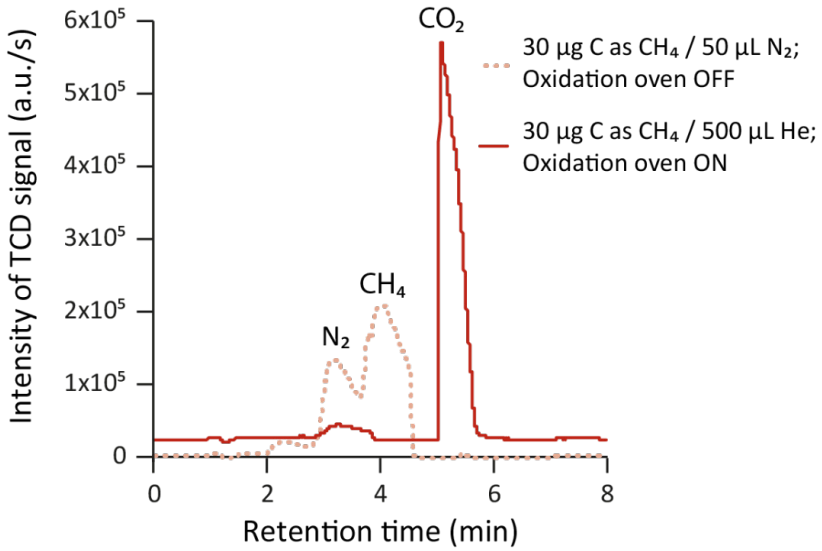

Fig. 10: Tests of the efficency of the oxidation oven

The light red dotted curve shows the N_2 and CH_4 peaks recorded by the TCD when 30 µg C (60 µL) as fossil CH_4 and 50 µL N_2 were injected and the oxidation oven was switched off (T = 400 °C). The overlap of the two peaks indicates co-elution of N_2 and CH_4. The dark red solid curve shows the CO_2 peak when 30 µg fossil CH_4 (peak area = 1.27×10^7 a.u.) and 500 µL He were injected and the oxidation oven was switched on (T = 1'000 °C). The CO_2 peak and a very small amount of N_2 as contamination from the previous injection were recorded by the TCD. Absence of a CH_4 peak indicates complete conversion of CH_4 into CO_2.

The efficiency of the oxidation oven was also checked at a higher carbon loading. To this end, 50 µg C in the chemical form of CH_4 was injected via the carrier loop (100 µL) simultaneously with 500 µL He via the sample loop. Only CO_2 was observed at a retention time between 4.9 and 5.7 min with the oxidation oven switched on, while the CH_4 peak was absent (3.5 to 4.5 min retention time) (Fig. 11), revealing complete oxidation of the 50 µg C as fossil CH_4 to CO_2. An additional injection was realised by loading 50 µg C as fossil CH_4 and 500 µL N_2 (instead of He) into the carrier and sample loop, respectively, to simulate oxidation of a gas sample coming from the corrosion experiment (N_2 atmosphere). The two CO_2 peak areas obtained between 4.9 and 5.7 min were identical for both injections (Fig. 11), thus proving 100 % efficiency of the oxidation oven under conditions representing a gas sample collected from the reactor.

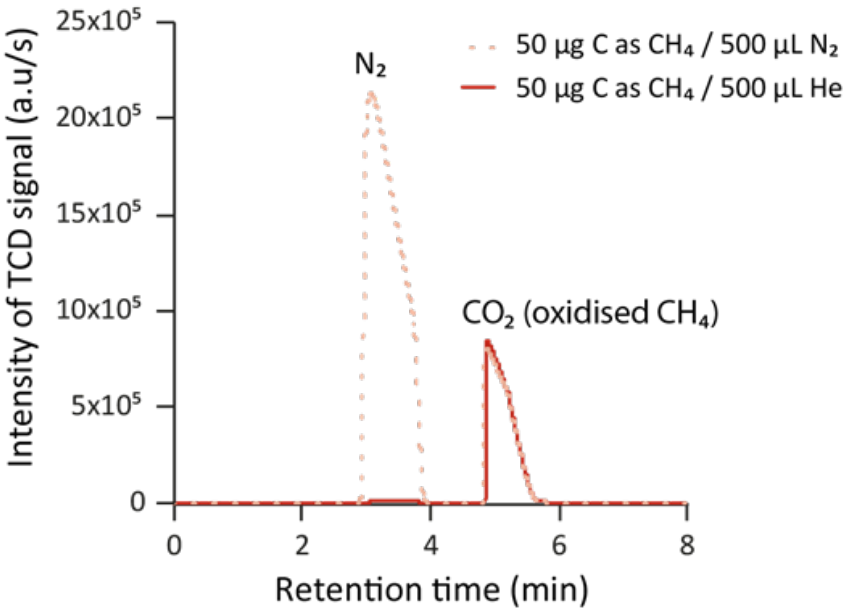

Fig. 11: Test of the efficiency of the oxidation oven with 50 µg C in the chemical form of fossil CH_4

Dark red solid line: TCD signal after an injection of 50 µg C as fossil CH_4 and 500 µL He. A single peak of CO_2 was recorded by the TCD between 4.9 and 5.7 min retention time. CH_4 normally present between 3.5 and 4.5 min was absent, proving complete oxidation of CH_4. Light red dotted line: TCD signal after an injection of 50 µg C as CH_4 and 500 µL N_2. The first peak (2.9 to 3.9 min retention time) corresponds to N_2 and the second one to oxidised CH_4 (CO_2) (4.9 and 5.7 min retention time). Complete oxidation of 50 µg C (100 µL) in the chemical form of CH_4 is confirmed as both CO_2 peaks from the two injections perfectly overlap and identical areas were recorded (2.220×10^7 a.u. and 2.223×10^7 a.u., respectively).

In addition to CH_4 conversion, the oxidation of C_2H_6 into CO_2 was tested. For this purpose, 60 µg C (60 µL loop) in the chemical form of fossil C_2H_6 were injected via the carrier loop (60 µL) simultaneously with He via the sample loop (500 µL) with the oxidation oven switched off (T = 400 °C), partially on (T = 700 °C) and on (T = 1'000 °C) (Fig. 12). In this case, the oxidised and un-oxidised forms of C_2H_6 obtained with the oxidation oven on and off, respectively, were separated only by a retention time of 0.1 min (Fig. 12). Co-elution (double peak) can be illustrated in case of partial oxidation at 700 °C. Nevertheless, we would expect a visible contribution of un-oxidised C_2H_6 to the peak detected with the oxidation oven switched on and a reduced peak height in these conditions if oxidation of C_2H_6 was incomplete at T = 1'000 °C. The absence of a double peak at T = 1'000 °C thus suggests complete oxidation of 60 µg C as fossil C_2H_6 into CO_2.

The efficiency of the oxidation oven was determined at different amounts of fossil C injected into the GC system, i.e. 20, 30, 40, 50, 60 and 100 µg C (Fig. 13). The linear increase of the CO_2 peak area detected by the TCD (corresponding to oxidised carbon compounds) and the amount of C injected corroborates that complete oxidation occurred at T = 1'000 °C at the given loadings.

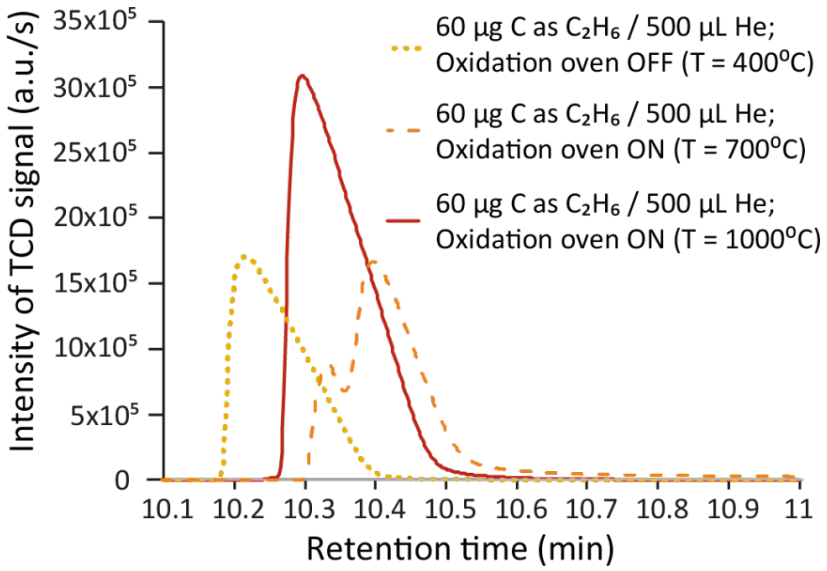

Fig. 12: TCD signal recorded by injecting 60 µg C as fossil C_2H_6 and and 500 µL He

Dotted yellow line: TCD signal with the oxidation oven switched off (T = 400 °C). Dashed orange line: TCD signal with the oxidation oven operated at reduced temperature (T = 700 °C). Solid red line: TCD signal with the oxidation oven switched on (T = 1'000 °C).

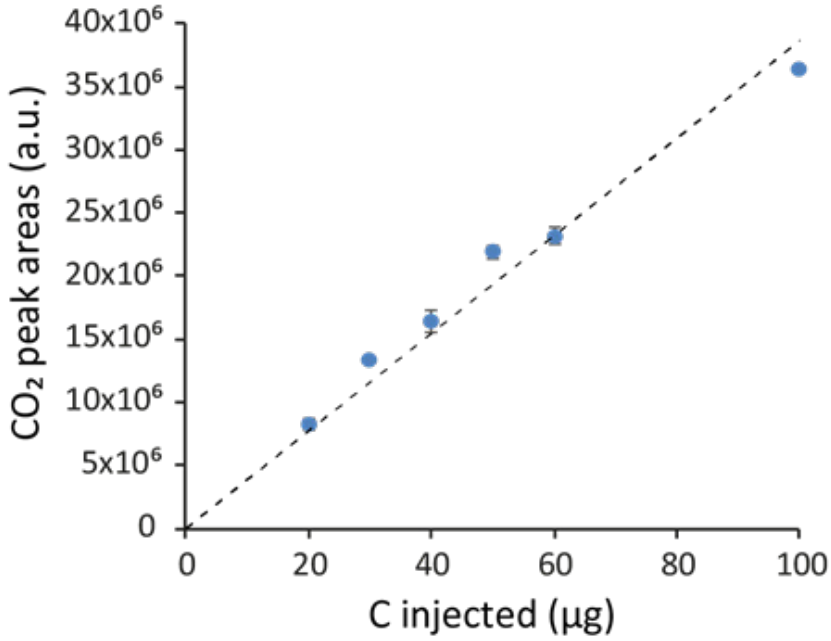

Fig. 13: Efficiency of the oxidation oven shown as the CO_2 peak area detected by the TCD (oxidised carbon compounds) as a function of the amount of C injected into the GC

The capacity of the Ni/Cu/Pt catalyst is limited and therefore regular regeneration was required to ensure optimal conditions during oxidation. Its maximal capacity was determined immediately after installation by sequentially injecting 20 µg C (40 µL loop) in the chemical form of fossil CH_4 via the carrier loop. The capacity was considered to be exhausted as soon as a small peak of CH_4 was recorded by the TCD between 3.5 and 4.5 min retention time in addition to the one of CO_2 between 5.0 and 5.7 min. To be able to detect the CH_4 peak in the TCD signal, 500 µL He (instead of N_2) was simultaneously injected via the sample loop. The percentage CO_2 was calculated using the ratio between the CO_2 and CH_4 peak areas (Fig. 14). Complete oxidation occurred up to 40 injections of 20 µg C as fossil CH_4. In the range between 40 to 55 injections, however, the efficiency of the oxidation oven gradually decreased to 98 %. At around 60 injections, the capacity was exhausted, and the efficiency dropped to 15 % within three injections (Fig. 14). The maximum capacity of the Ni/Cu/Pt catalyst was therefore estimated at 1'000 µg C, corresponding to 50 injections of 20 µg C.

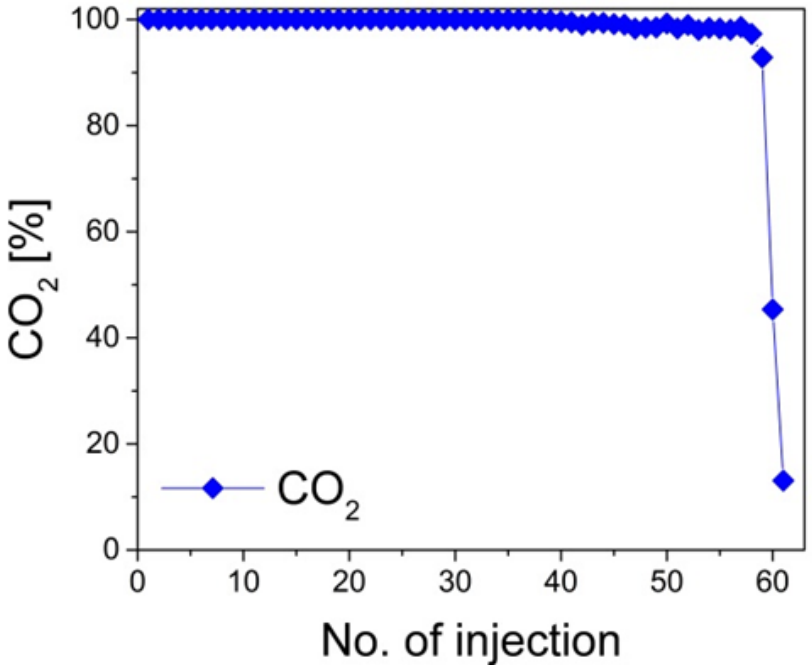

Fig. 14: Capacity test of the oxidation oven realised after its installation

For each injection, 20 µg C (40 µL loop) in the chemical form of fossil CH_4 were loaded into the carrier loop and 500 µL He into the sample loop. The % CO_2 was calculated from the ratio of the CO_2 and CH_4 peak areas.

The capacity of the oxidation reactor was tested a second time after three years of operation with the aim of checking the possibility of changes in performance with time. For this purpose, a series of consecutive injections with 50 µg C (100 µL loop) in the chemical form of fossil CH_4 and 500 µL He via the carrier and sample loops, respectively, were realised (Fig. 15).

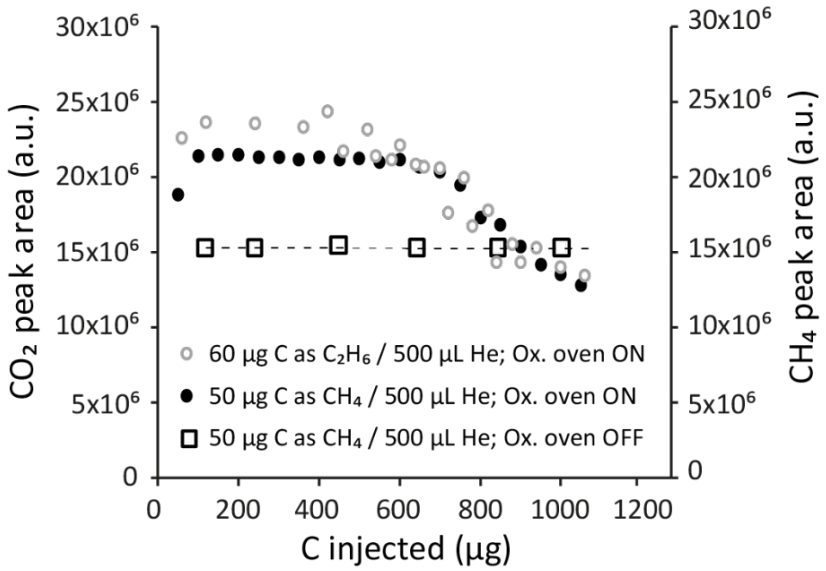

Fig. 15: Capacity tests of the oxidation oven realised after three years of operation

Black solid symbols: CO_2 peak areas determined by sequentially injecting 50 µg C (fossil CH_4) and 500 µL He with the oxidation oven switched on (T = 1'000 °C). Grey open symbols: CO_2 peak areas determined by injecting 60 µg C (fossil C_2H_6) and 500 µL He with the oxidation oven switched on (T = 1'000 °C). Black open squares: CO_2 peak areas determined by injecting 50 µg C (fossil CH_4) with 500 µL He with the oxidation oven switched off (T = 400 °C).

We anticipated that the limit of capacity of the oxidation oven would be indicated by small peaks of CH_4 recorded by the TCD between 3.5 and 4.5 min retention time in addition to the one of CO_2 observed between 5.0 and 5.7 min retention time. However, it was not possible to detect any CH_4 peak, even after injecting more than 2'500 µg C (data not shown), for currently unknown reasons. Nevertheless, a decrease of the CO_2 peak area was observed after injection of 600 µg C into the GC, which corresponds to a capacity of 480 µg C of the oxidation oven taking into account the efficiency of injection (80 %) at a splitless time of 1 min (Fig. 15).

The capacity was further tested by conducting a series of consecutive injections with 60 µg C as fossil C_2H_6 and 500 µL He. The same trend in the CO_2 peak areas was observed as for CH_4, thus confirming the limit of capacity of the oxidation oven at approximately 600 µg injected C (i.e. effective 480 µg C).

As a result of these tests, it was decided to regenerate the catalyst before each sample preparation. During sample preparations typically 7 injections were realised leading to a maximum loading of ~ 420 µg injected C.

4.2.2.3 Test of the reduction oven and the water trap

After the oxidation oven, the analyte stream passes through the reduction oven and the water trap (Fig. 3). The reduction oven removes any traces of O_2 and nitrous oxides (NO_x) with the help of a Cu catalyst. Residual water is then removed from the analyte stream by a water separator connected at the outlet of the reduction oven (Fig. 3). It consists of a NAFION™ membrane, which is continuously purged with a counter-current stream of dry He. A non-dispersive infrared (NDIR) detector detecting only CO_2 was connected to the GC-system after the TCD to test the efficiency of the reduction oven and the water trap. Two injections of 50 µg C (100 µL loop) in the chemical form of fossil CH_4 and 500 µL N_2 were realised with the reduction oven and water trap switched off (T = 50 °C; 500 µL He/min) as well as with the reduction oven and water trap switched on (T = 650 °C; 3 – 4 mL He/min) (Fig. 16).

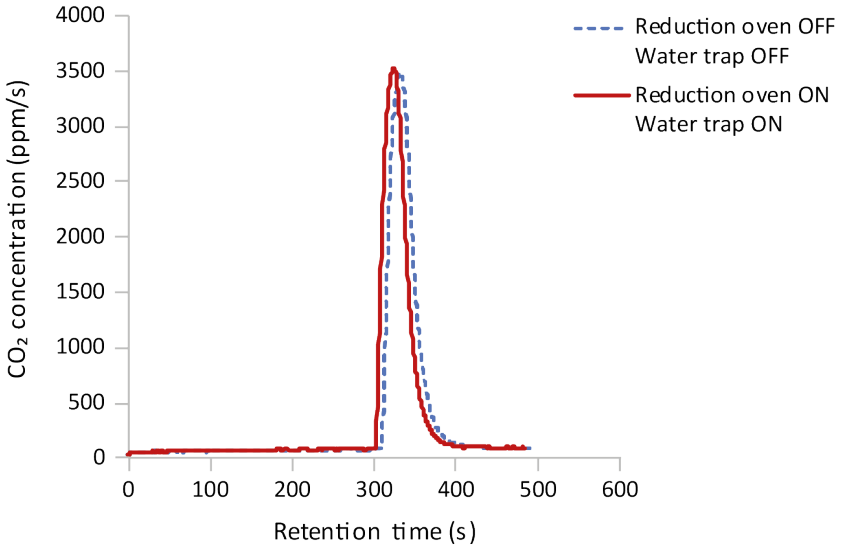

Fig. 16: Test of the operation of the reduction oven and the connected water trap using a NDIR detector

The latter detector records the CO_2 concentration (ppm) after the TCD and corresponds to the CH_4 injected in the GC and oxidised to CO_2 in the oxidation oven. Dashed blue line: CO_2 concentration recorded after an injection of 50 µg C as fossil CH_4 and 500 µL N_2 with the reduction oven and water trap switched off (peak area = 1.16×10^5 ppm). Solid red line: CO_2 concentration recorded after an injection of 50 µg C (100 µL; fossil CH_4) and 500 µL N_2 with the reduction oven and water trap switched on (peak area = 1.18×10^5 ppm). The areas of the two CO_2 peaks are identical within the uncertainty, revealing that the reduction oven and the water trap have no effect on the CO_2 recovery rate.

The two CO_2 peaks were found to be similar in shape and area (peak areas = 1.16×10^6 ppm with the reduction oven switched off and 1.18×10^6 ppm with the reduction oven switched on) (Fig. 16). Thus, operation of the reduction oven and the water trap does not have any impact on the amount of passing CO_2 and a complete carbon recovery was considered after these two devices.

The aforementioned tests of the performance of the GC system (including the GC, the oxidation and reduction ovens, the water trap and the TCD) reveal that the recovery rate of CO_2 is only affected by the injection mode. Setting the splitless time to 1 min during GC injection reduces carbon recovery to 80 %. A reduction of the splitless time from 2 to 1 min was required to avoid co-elution between HCs.

4.2.3 CO_2 recovery in the fraction collector

The fraction collector is composed of a collection valve and seven loops (#2 to #8) controlled by a custom-made software (Fig. 3). Note that loop #1 is only a by-pass. The collection valve starts and stops the trapping of the analytes of interest in the sampling loops in accordance with their retention time. The purge valve is used to flush each loop with He for several minutes before trapping to avoid any contamination with air. Hence, a loss of carbon could occur either in the collection valve, which needs to switch on correctly to allow the CO_2 to reach the loops or in the loops, in which CO_2 is stored.

4.2.3.1 Test of the collection valve

Gas-tightness of the collection valve was checked by loading the loops of the fraction collector with CO_2 and measuring the CO_2 concentration after release. To this end, the NDIR detector was connected after the TCD and subsequently after the by-pass (loop #1) or one of the sampling loops (loop #2 to #8) of the fraction collector (Fig. 17).

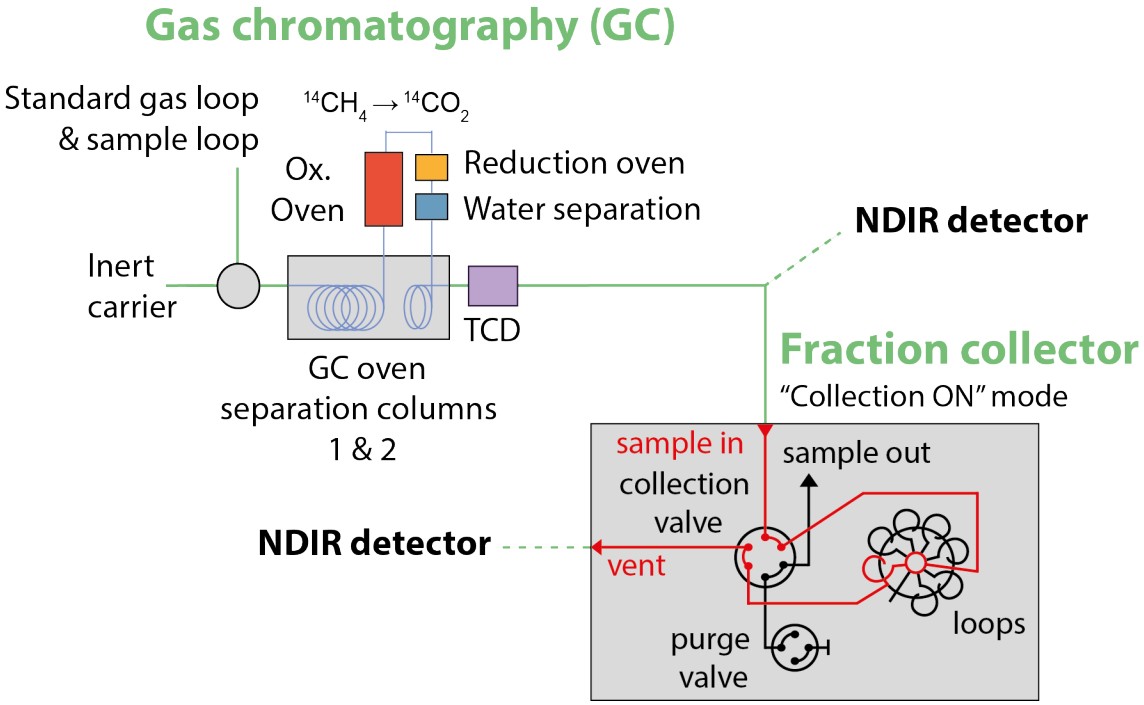

Fig. 17: Set-up for determining the carbon recovery in the fraction collector with a NDIR detector

The areas of the CO_2 peaks determined after the TCD and after the pass-by of the fraction collector were identical within the uncertainty (1.11×10^6 ppm and 1.10×10^6 ppm, respectively) (Fig. 18). A slightly lower area of the CO_2 peak was determined after loop #2 with a value of 1.06×10^6 ppm corresponding to 5 % reduction, which is within the uncertainty of the measurements (Fig. 18). The same tests were carried out with loops #3, #4, #5, #6, #7 and #8. All these loops showed a similar behaviour as observed for loop #2. For this reason, only the results for loop #2 are illustrated in Fig. 18. We concluded that the collection valve is gas-tight as the three CO_2 peak areas are almost identical after the TCD, by-pass and loops.

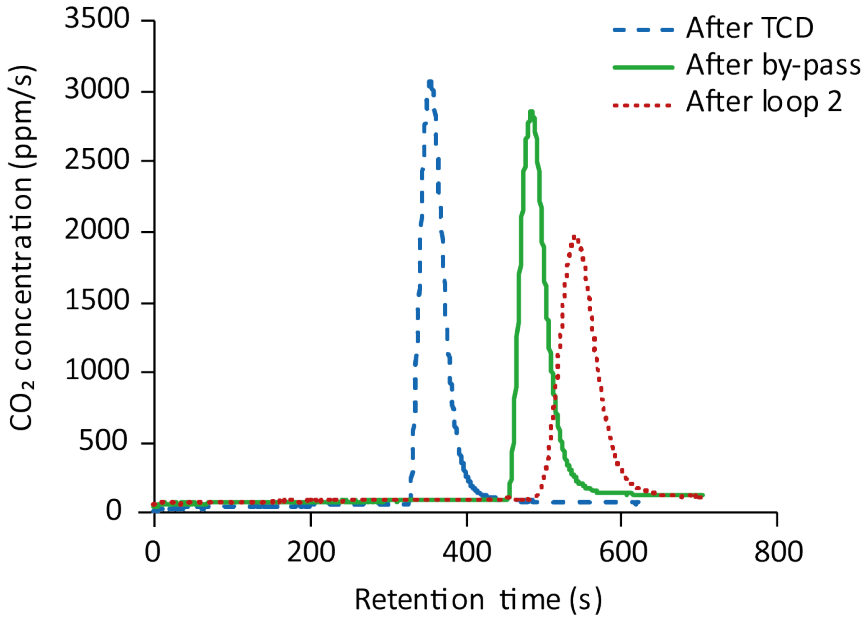

Fig. 18: Comparison between CO_2 peaks recorded by the NDIR detector after the TCD (dashed blue line, peak area = 1.11×10^6 ppm), the by-pass (solid green line; peak area = 1.10×10^5 ppm) and the loop #2 (dotted red line; peak area = 1.06×10^5 ppm)

Only CO_2 released from loop #2 is displayed as all the other loops showed a similar performance compared to loop #2.

4.2.3.2 Gas-tightness of the fraction collector loops

Gas-tightness of the fraction collector loops is an important criterion for an artefact-free realisation of CSRA in the case of gaseous carbon compounds. The loops need to be completely gas-tight for at least one day, which was the time lag between sample preparation and injection into the AMS. For example, each run for sample preparation lasts 20 min and the GC oven needs to cool down to 45 °C prior to the next injection. Overall, it takes about 3 h to load the seven loops with the analytes of interest. The transport of the fraction collector from the PSI Hot Laboratory to LARA (University of Berne) takes about 4 h, including the control for radioactive contamination of the fraction collector at PSI and its transfer by train to LARA. Eventually, it takes about 3 h to release the gas samples from the sampling loops one by one into the GIS and measure the ^{14}C concentrations by AMS. Hence, the sampling loops need to be gas-tight for at least 24 h.

Gas-tightness of each loop was checked by loading them with CO_2 and measuring the concentration released after different storage times with the NDIR detector. The recovery rate corresponds to the ratio of the initial amount of CO_2 to the measured concentration after release. For this purpose, 20 µg stable carbon (fossil CH_4) was injected via the carrier loop (40 µL) simultaneously with N_2 via the sample loop (500 µL) into the GC seven times in a row, trapped as CO_2 in the seven loops and then released after 1 h storage. This experiment was repeated a second time by applying a storage time of 3 days.

The CO_2 peak areas determined by the NDIR detector were compared loop-by-loop between the two experiments. The peak areas were found to be almost identical after 1 hour and 3 days storage (Fig. 19, Tab. 5). It is assumed that the areas obtained after 1 h storage correspond to 100 % recovery. Thus, the results suggest that all loops are gas-tight for at least a time period of 3 days. The CO_2 recovery determined after 3 days storage was slightly higher than 100 % for the loops #5, #7 and #8, which could be explained by a slightly lower flow rate of He applied during CO_2 release from these loops (Tab. 5). Furthermore, the shape of the CO_2 peaks was wider after 1 h storage than after directly passing through a loop due to a time-dependent effect on gas dispersion inside the loops (Figs. 18 and 19).

Tab. 5: CO_2 peak areas recorded by the NDIR detector after 1 h and 3 days of CO_2 storage in the sampling loops

The percentage of CO_2 recovery was calculated from the ratio of the CO_2 peak areas measured after 3 days and after 1 h.

No of loop	**Peak area after 1 h storage** [ppm]	**Peak area after 3 days storage** [ppm]	**Recovery** [%]
#2	1.34×10^5	1.33×10^5	99
#3	1.71×10^5	1.69×10^5	99
#4	1.59×10^5	1.58×10^5	99
#5	1.64×10^5	1.66×10^5	101
#6	1.60×10^5	1.58×10^5	99
#7	1.36×10^5	1.37×10^5	101
#8	1.59×10^5	1.71×10^5	107

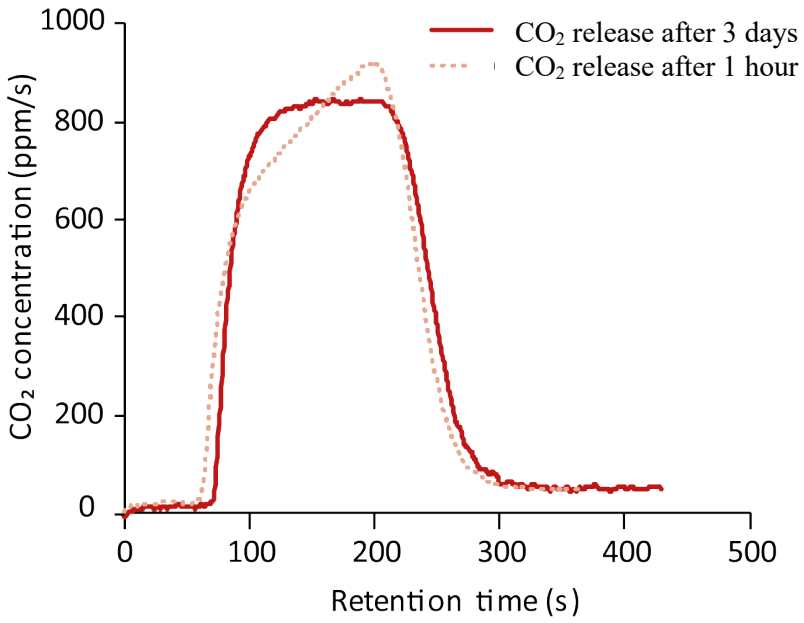

Fig. 19: CO_2 concentrations released after 1 h (dotted light red line; peak area = 1.34×10^5 ppm) and 3 days (solid dark red line; peak area = 1.33×10^5 ppm) of CO_2 storage in loop #2

Only the results for loop #2 are displayed because all other sampling loops showed a similar behaviour. CO_2 concentrations were recorded by a NDIR detector connected after each of the sampling loops of the fraction collector.

An additional and independent test was performed to confirm gas-tightness of the loops. To this end, each of the sampling loops was subjected to a pressure of 22 psi of He, using the manometer of the fraction collector. The pressure was recorded immediately after pressurising the loops (day = 0 in Tab. 6) and after 1, 3, 7 or 14 days storage (Tab. 6, Fig. 20). The pressure did not change up to 14 days for all loops except loop #5. The pressure of loop #5 steadily decreased with time, reaching a minimum of 8 psi after 14 days (Tab. 6, Fig. 20). The reason for this pressure loss in loop #5 is presently not known, particularly in the light of the tests carried out with CO_2 (Tab. 6), which clearly showed gas-tightness of loop #5 (Tab. 5).

Tab. 6: Gas-tightness test of the sampling loops by pressurising at 22 psi

Loop	**Volume** [mL]	**Pressure** [psi]	**Day**				
			0	**1**	**3**	**7**	**14**
#2	25	22	22	22	22	22	22
#3	25	22	22	22	22	22	22
#4	25	22	22	22	22	22	22
#5	25	22	22	20	18	14	8
#6	25	22	22	22	22	22	22
#7	60	22	22	22	22	22	22
#8	60	22	22	22	22	22	22

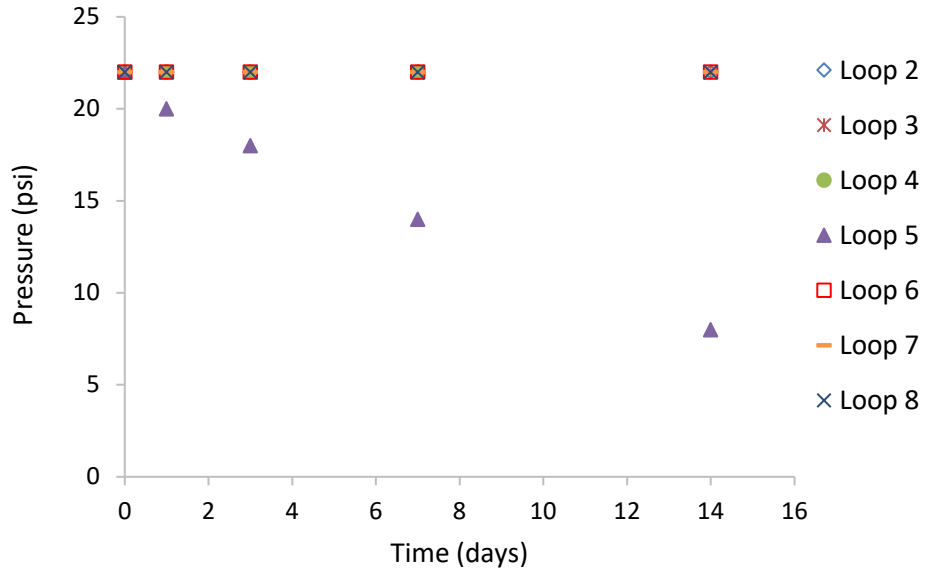

Fig. 20: Pressure measured in the loops after 14 days of He storage.

In summary, the collection valve and sampling loops of the fraction collector are gas-tight and allow CO_2 storage for a period of at least 3 days.

After all the tests performed with the GC-TCD system including the fraction collector, we infer that the overall recovery of fossil CH_4 (and other HCs) is equal to 80 % due to the chosen injection mode. As 20 µg ^{12}C was recommended by LARA for reliable ^{14}C measurements by AMS, it was decided to use a carrier loop (100 µL) with a capacity of 50 µg C. This should result in the release of 40 µg stable carbon into the GIS of the AMS taking into account the carbon recovery of the GC-TCD system and fraction collector. The amount of 50 µg stable carbon was chosen in order to inject a sufficient amount of ^{12}C into the MICADAS and be able to make more than seven injections without exhausting the capacity of the oxidation oven.

4.2.4 AMS measurements with fossil CH_4

Carbon recovery in the GIS was checked by performing tests with fossil CH_4. To this end, 50 µg C as fossil CH_4 and 500 µL N_2 were sequentially injected into the GC via the carrier and sample loops, respectively. Fossil CH_4 was oxidised to CO_2 in the oxidation oven and trapped in the seven sampling loops of the fraction collector. Then, CO_2 was released from the different loops into the GIS and further injected into the MICADAS for ^{14}C AMS measurements. The aforementioned recovery tests with the GC-TCD system and fraction collector have shown that 40 µg stable carbon out of the 50 µg stable carbon injected into the GC should be released into the GIS. It is possible to verify this assumption as the syringe of the GIS records the amount of CO_2 released into the AMS source. The syringe has a known volume expanding in accordance with the CO_2 released from the zeolite trap (Fig. 5). The results showed that it collected between 18 and 34 µg stable carbon out of the 50 µg stable carbon injected into the GC, corresponding to between 36 and 68 % carbon recovery (Tab. 7). This indicates that a portion of stable carbon was lost during injection into the AMS. Two reasons were considered to explain this reduction in carbon recovery. It might be explained by the too short collection time during CO_2 release from the fraction collector loops and trapping by the GIS zeolite trap, while it should be noted that the trapping time was

properly defined according to the geometry of each loop and the He flow rate applied to purge the CO_2 from the loops into the GIS (i.e. between 150 and 300 s). For instance, the trapping time was doubled for loops #7 and #8 having a volume 2.4 times larger than the other loops. Another explanation might be the limited efficiency of the CO_2 trap of the GIS to recover quantitatively CO_2 released from the sampling loops. In any case, by injecting between 18 and 34 µg stable carbon into the MICADAS source, the ^{12}C-related current detected by the Faraday cup was always > 5 µA (Tab. 8), which is above the minimum current of 2 µA required for robust ^{14}C AMS measurements. No further attempts were made to unravel the reason for the reduced carbon recovery in the GIS-AMS system because the ^{14}C measurements were highly reproducible and resulted in a mean value of the background of 0.012 $F^{14}C$ with a very low standard deviation of 0.008 $F^{14}C$ (Tab. 7).

To characterise the different $F^{14}C$ signatures of two gas sources and detect a potential cross contamination during the successive release of samples having different ^{14}C contents, a second test was carried out by sequentially injecting 50 µg C as fossil CH_4/500 µL N_2 and 50 µg C as modern CH_4/500 µL N_2. Fossil and modern CH_4 were trapped one after the other in the different loops of the fraction collector and released into the AMS. The measurements show that, as expected, fossil and modern CH_4 have distinct $F^{14}C$ signatures, i.e. 0.032 ± 0.007 $F^{14}C$ and 1.010 ± 0.011 $F^{14}C$, respectively (Tab. 9). The low standard deviations show a good reproducibility of the measurements and suggest that no cross contamination occurred when different ^{14}C contents were successively injected into the AMS (Tab. 9).

While the same conditions had been applied for the sample preparation (i.e. GC separation and fraction collector sampling), the overall carbon recovery measured by the syringe of the GIS tended to be better in this second test, i.e. ranging from 44 to 78 % (Tab. 8) as compared to the first one (Tab. 7). These slight differences could be explained by instabilities of the GIS/MICADAS systems and/or by a slightly different He flow passing through the sampling loops while CO_2 was purged into the GIS.

Tab. 7: ^{14}C AMS readings when 50 µg C in the chemical form of fossil CH_4 was injected into the GC, oxidised to CO_2, trapped by the sampling loops of the fraction collector and released into the AMS through the GIS

The $F^{14}C$ values were corrected with the AMS blank determined by injecting CO_2 directly from a gas bottle (fossil CO_2) at the beginning of each sequence. The weight of total carbon (stable carbon + ^{14}C) trapped in the GIS and released in the AMS source was manometrically measured by the GIS and allowed the calculation of the overall carbon recovery.

No. of loop	**^{12}C-related current** [µA]	**$F^{14}C$**	**Uncertainty** [%]	**Weight of total carbon detected by AMS** [µg]	**Total carbon recovery** [%]
Blank	5.91	0.010	8.3	-	-
#2	5.72	0.021	8.0	21	42
#3	6.05	0.011	13.4	18	36
#4	5.60	0.003	45.5	34	68
#5	5.09	0.029	6.5	27	54
#6	5.47	0.007	20.3	28	56
#7	5.65	0.010	17.4	23	46
#8	5.81	0.007	22.1	33	66

Tab. 8: ^{14}C AMS readings after injections of 50 µg C in the chemical forms of fossil and modern CH_4, respectively, as carrier into the GC system

The $F^{14}C$ values were corrected with the AMS blank determined at the beginning of each sequence by injecting CO_2 directly from a gas bottle into the GIS. The weight of total carbon was manometrically measured by the GIS and allowed the calculation of the overall carbon recovery. The reference $F^{14}C$ value of the modern CH_4 is 1.024 ± 0.003 (Espic et al. 2019).

Sample	**^{12}C-related current** [µA]	**$F^{14}C$**	**Uncertainty** [%]	**Weight of total carbon detected by AMS** [µg]	**Total carbon recovery** [%]
Blank	6.81	0.011	7.6	-	-
loop #2 – fossil CH_4	5.15	0.038	7.3	26	51
loop #3 – modern CH_4	4.76	1.005	1.1	39	78
loop #4 – modern CH_4	5.67	1.017	1.1	32	64
loop #5 – fossil CH_4	5.84	0.035	5.9	32	64
loop #6 – modern CH_4	5.17	0.997	1.1	31	62
loop #7 – modern CH_4	6.17	1.023	1.1	24	48
loop #8 – fossil CH_4	6.32	0.024	8.9	22	44

In both tests, the loops #2, #5 and #8 were loaded with fossil CH_4 in the same analytical conditions and therefore, these data can directly be compared (Tab. 9). It was observed that the ^{12}C current was stable (average of 5.6 ± 0.4 µA), indicating the possibility of conducting consistent $F^{14}C$ measurements over time (Tab. 9). Moreover, loop #5, found to potentially leak according to the test with pressurised He, showed neither a lower ^{12}C current nor a lower recovery as compared to loops #2 and #8 (Tab. 9). The $F^{14}C$ values obtained for loop #5 were even consistent with those obtained for loops #2 and #8 (Tab. 9), clearly revealing that loop #5 was not leaking and can further be used for gas trapping.

Tab. 9: Results from two distinct runs conducted with the same loops within one month: ^{12}C-related current, $F^{14}C$ values and the overall total carbon recovery of fossil CH_4

No. of loop	**Run**	**^{12}C-related current**		**$F^{14}C$**		**Weight of total carbon injected into the AMS**	**Total carbon recovery**	
		Value [µA]	**σ** [µA]	**Value**	**σ**	[µg]	**Value** [%]	**Σ** [%]
#2	1	5.72	0.40	0.021	0.012	21	42	7
	2	5.15		0.038		26	51	
#5	1	5.09	0.53	0.029	0.005	27	54	7
	2	5.84		0.035		32	64	
#8	1	5.82	0.36	0.007	0.012	33	66	15
	2	6.32		0.024		22	45	

4.3 Preliminary results from the corrosion experiment with irradiated steel: Demonstration of feasibility of the analytical approach for ^{14}C detection

This section presents selected results from the samplings of the corrosion experiment with irradiated steel performed after 1'114 days of corrosion. The aim is to exemplarily illustrate the application of the analytical developments made to quantify ^{14}C in the liquid and gas phase of the corrosion experiment. To this end, 7 mL solution and 50 mL gas phase were sampled from the reactor after 1'114 days of corrosion, according to the sampling procedure previously described in Section 2.2. A summary of all results obtained from the start of the corrosion experiment with irradiated steel will be published in a separate report.

4.3.1 Determination of $TO^{14}C$ and $TI^{14}C$

Direct measurements of $TO^{14}C$ (d-$TO^{14}C$) and $TI^{14}C$ were carried out in the liquid phase sampled after 1'114 days corrosion (method described in Section 3.6). The $F^{14}C$ measurements were corrected with the blank, i.e. $F^{14}C$ determined for ACW, the amount of stable carbon added to the sample for reliable ^{14}C AMS measurements and the final volume injected into the GIS (i.e. 1.25 mL). The $F^{14}C$ measurements, made in duplicates, showed reproducible data with small standard deviations (i.e. 170.54 ± 2.11 for d-$TO^{14}C$ and 73.47 ± 1.99 for $TI^{14}C$; Tab. 10).

Dissolved ^{14}C-bearing organic carbon was determined in solution after cartridge treatment (p-$TO^{14}C$) (method described in Section 3.7.1). The $F^{14}C$ value was corrected for the blank, the amount of stable carbon added, and the final volume injected into the EA (i.e. 10 µL).

Comparison of the results from direct and indirect $TO^{14}C$ measurements (d-$TO^{14}C$ and p-$TO^{14}C$) revealed a difference in the $F^{14}C$ of almost two orders of a magnitude (i.e. 170.54 for d-$TO^{14}C$ and 2.80 p-$TO^{14}C$; Tab. 10). This can be explained by the volumes of solution injected in the GIS and EA, which differed by a factor of ~ 100 (i.e. 1.25 mL for the GIS and 10 µL for the EA). In particular, however, the $F^{14}C$ values recorded for d-$TO^{14}C$ were well above the linear dynamic range of the AMS (i.e. 0.06-50 $F^{14}C$; Section 4.1.3), giving rise to ^{14}C contaminations in the GIS and MICADAS source. As a result, it was decided to reduce the amount of solution injected into the GIS by a factor of 10 (i.e. 0.125 mL instead of 1.25 mL) in future analyses in order to stay within the dynamic range and avoid ^{14}C contamination.

Tab. 10: $F^{14}C$ values of $TO^{14}C$ and $TI^{14}C$ of the liquid phase sampled after 1'114 days of alkaline anoxic corrosion of irradiated steel

$F^{14}C$ values were corrected with respect to the blanks and the experimental parameters (see text). $TO^{14}C$ was measured directly (d-$TO^{14}C$) and after Ag/Ba/H cartridge pre-treatment (p-$TO^{14}C$).

Samples	**$F^{14}C$** [$F^{14}C$]	**After blank correction** [$F^{14}C$]	**Average** [$F^{14}C$]	**σ** [$F^{14}C$]
d-$TO^{14}C$-1	185.51	172.64	170.54	2.11
d-$TO^{14}C$-2	179.15	168.43		
p-$TO^{14}C$	2.30	2.80	2.80	-
$TI^{14}C$-1	77.51	71.47	73.47	1.99
$TI^{14}C$-2	80.90	75.46		

4.3.2 Quantification of the single aqueous ^{14}C-bearing compounds

CSRA of the liquid phase was performed to quantify the ^{14}C-bearing carboxylic acids in solution, i.e. FA, AA, MA, OA and LA (method see Sections 3.7.2 and 3.7.3). The compounds were separated by IC prior to ^{14}C quantification by AMS. Furthermore, the freeze-drying process was applied to be able to quantify ^{14}C in the dynamic range of AMS. The $F^{14}C$ values determined by AMS were corrected for the ^{14}C background (0.06 $F^{14}C$) previously determined by Cvetković et al. (2018c) and the recovery after the Ag/Ba/H cartridge pre-treatment. The $F^{14}C$ values were above the LOD of the AMS (0.06 ± 0.02 $F^{14}C$) in case of ^{14}C-bearing FA, AA, and MA (Tab. 11). However, they were close or even below the LOD in case of ^{14}C-bearing OA and LA. In addition, we observed some outliers. For example, the $F^{14}C$ values of the last replicate of AA, the first two measurements of MA as well as the first measurement of OA were one order of magnitude higher than those of the other samples because of a ^{14}C contamination (values indicted in italic in Tab. 11). Note that all the samples were treated at the same time in exactly the same way and, therefore, we have not been able to identify the source of ^{14}C contamination to date. Hence, the outliers have been omitted in the calculations of the mean value and standard deviation. As a result of this observation, it was decided to avoid the freeze-drying step in future analyses of single compounds and directly determine the ^{14}C concentration after fractionation by IC by the oxidative treatment of the organic carbon compounds described in Sections 3.6 and 3.7.2. CSRA based on IC fractionation combined with wet oxidation will allow larger volumes of solution to be analysed, which results in $F^{14}C$ values well above the LOD and therefore does not require a pre-concentration step by freeze-drying.

FA and AA were found to be the dominant ^{14}C-bearing carboxylic acids present in solution in the sampling carried out in the first year of the corrosion experiment (Cvetković et al. 2018a). In addition, ^{14}C-bearing LA was quantified at concentrations close to the LOD of the method. The concentration of ^{14}C-bearing MA was below the LOD in these earlier samplings. However, in the current sampling after 1'114 days of corrosion, we observed for the first time a substantial concentration of ^{14}C-bearing MA. Nevertheless, this finding should be judged with caution because only one replicate was available, which could further be affected by cross contamination coming from the two previous injected samples having high $F^{14}C$ values (Tab. 11).

Tab. 11: $F^{14}C$ of the single ^{14}C-bearing carboxylic acids in solution after 1'114 days of alkaline anoxic corrosion of irradiated steel

$F^{14}C$ values were corrected with respect to the blanks and the experimental parameters (see text). Outliers affected by ^{14}C contamination during the freeze-drying step and not taken into account in the calculations of the ^{14}C concentrations are indicated in italic.

Samples	**$F^{14}C$** [$F^{14}C$]	**After corrections** [$F^{14}C$]	**Mean value** [$F^{14}C$]	**σ** [$F^{14}C$]
FA-1	0.37	0.31	0.27	0.07
FA-2	0.31	0.25		
FA-3	0.31	0.25		
AA-1	0.40	0.34	0.37	0.03
AA-2	0.47	0.41		
AA-3	*2.17*	*2.11*		
MA-1	*4.09*	*4.03*	0.79	-
MA-2	*7.13*	*7.07*		
MA-3	0.85	0.79		
OA-1	*7.10*	*14.14*	0.35	0.18
OA-2	0.25	0.44		
OA-3	0.16	0.26		
LA-1	0.22	0.16	0.17	0.04
LA-2	0.26	0.20		
LA-3	0.23	0.17		
Sum CAs			**1.89**	

4.3.3 Identification of the hydrocarbons in the gas phase

According to the previous study of Cvetković et al. (2018b), it was expected that small HCs ranging from one (CH_4) to four (C_4H_{10}) carbon atoms are present in the gas phase at detectable concentrations. Thus, several GC-MS scans were carried out to identify these carbon compounds of interests in the gas sampled from the reactor. The compounds were identified according to their specific ion fragments and retention times (Fig. 21). Note that MS only allows HCs to be detected at concentrations in the ppb to ppm concentration range. Therefore, only the identification of stable carbon compounds was possible by MS rather than the detection of the ^{14}C-bearing carbon compounds. Only H_2 (specific fragments of 5 m/z, present at 2.5 min), CH_4 (specific fragments of 15 and 16 m/z, present at 4.4 min) and C_2H_6 (specific fragments of 29 and 30 m/z, present at 10.45 min) were identified in the gas phase of the reactor after 1'114 days of reaction (Fig. 21). CH_4 seems to be the dominant HC in the gas as its peak area was five times higher than that of C_2H_6 (Fig. 21). Even if it is expected that the peaks visible in the MS chromatogram are mainly composed of stable carbon compounds, we assumed that the concentrations of stable HCs could be an indication for the proportion of the ^{14}C-bearing HCs in the gas phase during corrosion of

irradiated steel. Hence, we infer from the analysis of stable carbon compounds that CH_4 might be an important ^{14}C-bearing species, while C_2H_6 is less abundant. The presence of H_2 is expected as it is the main gaseous species formed during alkaline anoxic corrosion of steel.

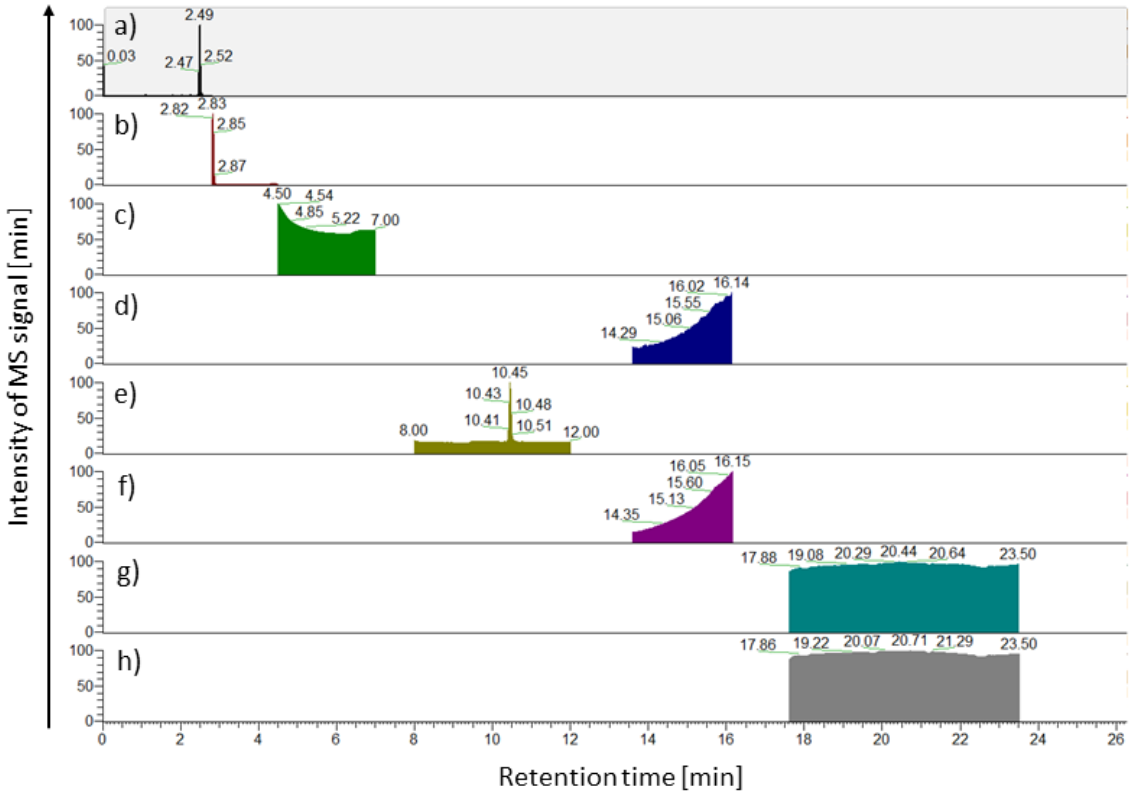

Fig. 21: Chromatograms of the gas sampled from the reactor after 1'114 days of corrosion

a) Chromatogram with the specific mass fragment of 5, corresponding to the peak of H_2 that arrives at 2.5 min retention time. This molecular ion is actually the result of the protonation by H^+ of the carrier gas (He; Varlet et al. 2013). b) Chromatogram with the specific mass fragments of 15 and 16, showing the presence of CH_4 at 2.83 min. c) Chromatogram with the specific mass fragment of 28 and 29 at 4.4 min, characteristic of CO but absent in the sample. d) Chromatogram with the specific mass fragments of 25 and 26 at 15.29 min, typical of C_2H_4 but absent in the sample. e) Chromatogram with the specific mass fragments of 29 and 30, revealing the presence of C_2H_6 at 10.45 min. f) Chromatogram with the specific mass fragments of 29 and 43 at 15.71 min, characteristic of C_3H_8 but absent in the sample. g) Chromatogram with the specific mass fragments of 41 and 42 at 20.4 min, typical of C_3H_6 but absent in the sample. h) Chromatogram with the specific mass fragments of 43 and 58 at 22 min, characteristic of C_4H_{10} but absent in the sample.

4.3.4 Quantification of $^{14}CH_4$ in the gas phase

We carried out scoping calculations prior to the analysis of $^{14}CH_4$ with the aim of optimising the sample preparation for the ^{14}C AMS measurements of HCs. The assessment was necessary to make sure that the expected ^{14}C concentration of the gaseous compounds fall in the linear dynamic range of the AMS (i.e. ~ 0.06 to ~ 50 $F^{14}C$). The ^{14}C concentration was estimated based on the corrosion rates of irradiated steel during the first two years of experiment (Cvetković et al. 2018a), time of corrosion, surface area of the two irradiated steel nuts mounted in the reactor, their ^{14}C content and the C amount injected into the GC via the sampling loops. The calculations showed that the ^{14}C concentration in the gas phase should range between 7 and 8 $F^{14}C$ after 1'000 days of reaction, taking into account the dilution of the gas phase after each sampling by N_2. Thus, in principle, no further dilution of the gas was necessary, as the expected ^{14}C concentrations should be in the linear dynamic range of the AMS.

The correctness of the calculations was checked by trapping CH_4 in diluted and non-diluted gas samples. To dilute the gas by a factor of 100, 1 mL volume of the gas sampled from the sampling tube was collected with a gas-tight syringe, injected into a gas bag, which was then filled with N_2 to a volume of 100 mL. To dilute the gas by a factor of 10, a similar method was applied except that 1 mL of the sample was diluted in the gas bag with only 10 mL N_2. Afterwards, 40 µL gas mixture were sampled from the gas bag and injected into the sample loop while 50 µg C as fossil CH_4 were injected into the carrier loop. The mixture sample/carrier was simultaneously injected into the GC, subjected to chromatographic separation, oxidised to CO_2 and trapped in the different sampling loops of the fraction collector. CO_2 diluted by a factor of 100 was stored in loops #2 and #3, CO_2 diluted by a factor of 10 was collected in loops #4 and #5, and CO_2 from the undiluted gas sample was trapped in loops #6 and #7 (Tab. 12). The fraction collector was transferred to LARA and all the loops were injected into the MICADAS via the GIS as described previously (Sections 3.9.1 and 3.9.2).

Tab. 12: Determination of $^{14}CH_4$ in gas sampled from the reactor after 1'114 days of corrosion

For the preparation of the AMS samples trapped in loop #2, the gas was diluted by a factor of 100. Loop #3 was not analysed as the value obtained for loop #2 was below the LOD and it was its duplicate. For the preparation of the AMS samples trapped in loops #4 and #5, the gas was diluted by a factor of 10. The samples in loops #6 and #7 were prepared from the undiluted gas phase.

No. of loop	**Sample**	**^{12}C-related current** [µA]	**$F^{14}C$**		**Weight of total carbon** [µg]	**Recovery of total carbon** [%]
			Value	**Error** [%]		
Blank	AM blank	2.44	0.033	7.9	n.d.	n.d.
#2	100 times diluted gas – CH_4 as carrier	2.19	0.049	11.1	29.1	78
#4	10 times diluted gas – CH_4 as carrier	2.14	0.070	8.2	37.2	99
#5	10 times diluted gas – CH_4 as carrier	2.37	0.077	7.5	36.6	98
#6	no dilution of gas – CH_4 as carrier	1.97	0.504	2.3	37.3	99
#7	no dilution of gas – CH_4 as carrier	3.08	0.544	1.9	22.4	60

n.d.: not determined

The measurements showed that the $F^{14}C$ was very low in the loops containing the diluted oxidised $^{14}CH_4$ (dilution by a factor of 10 or 100) (Tab. 12). Indeed, the values were below 0.1 $F^{14}C$ and hence close to the LOD (0.03 ± 0.01 $F^{14}C$). As the $F^{14}C$ value of loop #2 was close to the LOD and loop #3 was its duplicate, it was not even analysed by AMS. The ^{14}C AMS analyses of undiluted oxidised $^{14}CH_4$ trapped in loops #6 and #7 showed $F^{14}C$ values ~ 0.51 $F^{14}C$, i.e. well above the LOD. This finding therefore confirmed that no further dilution of the gas sampled from the reactor was required for ^{14}C AMS measurements.

4.3.5 Quantification of $^{14}C_2H_6$ in the gas phase

C_2H_6 was identified by GC-MS in the gas sampled from the reactor. The chromatogram showed that the peak of CH_4 was about five times higher than the one of C_2H_6, thus suggesting a higher concentration of CH_4 compared to C_2H_6. For this reason, the gas sample was not diluted for the AMS measurements of ^{14}C-bearing C_2H_6. The gas sample was directly injected into the GC via the 40 µL sample loop simultaneously with 60 µg C in the chemical form of fossil C_2H_6 via the 60 µL carrier loop. C_2H_6 was chromatographically separated, oxidised to CO_2, and trapped in loops #4, #5 and #6. As no blank values were available for fossil C_2H_6 carrier gas, 60 µg C as fossil C_2H_6 and 500 µL N_2 were simultaneously injected via the carrier and sample injection loops, chromatographically separated, oxidised to CO_2, and trapped in the sampling loops #2 and #3 of the fraction collector. The AMS results showed similar $F^{14}C$ values for the C_2H_6 blanks and samples (~ 0.16 $F^{14}C$) (Tab. 13). This finding suggests that the fossil C_2H_6 carrier gas contains a significant portion of ^{14}C, which increases the blank value and makes the quantification of $^{14}C_2H_6$ impossible. Nevertheless, this indicates that the $^{14}C_2H_6$ concentration in the gas phase of the rector was very low after three years of alkaline anoxic corrosion of irradiated steel (below the LOD, ~ 0.16 $F^{14}C$).

Tab. 13: Determination of $^{14}C_2H_6$ in undiluted gas sampled from the reactor and fossil C_2H_6 carrier

No. of loop	**Sample**	**^{12}C-related current** [µA]	**$F^{14}C$**		**Weight of total carbon** [µg]	**Recovery of total carbon** [%]
			Value	**Error** [%]		
	blank	5.94	0.055	3.1	n.d.	n.d.
#2	N_2 in sample loop – fossil C_2H_6 as carrier	5.34	0.267	2.8	20.9	42
#3	N_2 in sample loop – fossil C_2H_6 as carrier	4.20	0.130	3.9	26.1	51
#4	undiluted gas – fossil C_2H_6 as carrier	3.82	0.111	4.2	21.5	42
#5	undiluted gas – fossil C_2H_6 as carrier	3.82	0.105	4.4	27.3	54
#6	undiluted gas – fossil C_2H_6 as carrier	3.48	0.086	5.1	n.d.	n.d.

n.d.: not determined

4.3.6 Determination of the total ^{14}C content in the gas phase

$TG^{14}C$ was determined with the aim of checking whether other ^{14}C-bearing gaseous compounds in addition to $^{14}CH_4$ and $^{14}C_2H_6$ might be present in the gas phase of the reactor. For this purpose, 40 µL gas sample was injected into the GC via the sample loop together with 50 µg C as fossil CH_4 via the carrier loop (100 µL). The mixture passed through a fused silica capillary, instead of the GC column 1, was oxidised to CO_2 in the oxidation oven and trapped in loops #4, #5, #6 of the fraction collector (Tab. 14). In this way, the carbon compounds in the gas phase were not separated based on different retention times but they arrived at the same time in the oxidation oven. After oxidation of the total carbon content, CO_2 was trapped in the sampling loops of the fraction collector. Blanks were also determined by injecting 500 µL N_2 and 50 µg C as fossil CH_4 via the sample and carrier injection loops, respectively, and trapping CO_2 in the sampling loops #2, #3 and #7 (Tab. 14). The $F^{14}C$ in the gas phase was determined to be ~ 0.51 $F^{14}C$. Hence, the total ^{14}C content in the gas phase agrees well with the concentration of $^{14}CH_4$ (Tabs. 12 and 14) confirming that methane is the dominant ^{14}C-bearing HC in the gas phase of the reactor.

Tab. 14: $F^{14}C$ values of the total gas fraction sampled from the reactor

Aliquots of the gas phase were injected into the GC without further dilution.

No. of loop	**Sample**	**^{12}C-related current** [µA]	**$F^{14}C$**		**Weight of total carbon** [µg]	**Recovery of total carbon** [%]
			Value	**Error** [%]		
	blank	6.09	0.014	7.6	n.d.	n.d.
#2	N_2 in sample loop – fossil CH_4 as carrier	4.90	0.012	16.1	n.d.	n.d.
#3	N_2 in sample loop – fossil CH_4 as carrier	4.00	0.014	14.9	n.d.	n.d.
#4	undiluted gas – fossil CH_4 as carrier	5.67	0.507	1.3	n.d.	n.d.
#5	undiluted gas – fossil CH_4 as carrier	5.12	0.513	1.4	31.4	84
#6	undiluted gas – fossil CH_4 as carrier	4.99	0.523	1.4	30.0	80
#7	N_2 in sample loop – fossil CH_4 as carrier	5.32	0.035	10.1	25.0	67

n.d.: not determined

4.4 Example: ^{14}C quantification after 1252 days of corrosion of irradiated steel

In Tab. 15, the complete set of ^{14}C measurements by AMS are exemplarily shown for the liquid and gaseous phases sampled after 1'252 days of corrosion of irradiated steel. Note that the compiled ^{14}C concentrations correspond to the actual concentrations in the reactor, which had not been corrected for dilution of the two phases since the start of the experiment by sampling and reinjection of fresh gas and solution to keep the volumes constant with time.

The results of the AMS measurements are presented in terms of fraction modern ($F^{14}C$) as it is the unit of the radiocarbon measurements and, after conversion, in molarity (mol ^{14}C/L) of the leaching solution and in moles per volume (mol ^{14}C/L) of the gas phase. Taking all the experimental correction parameters, volume of sample solution and amount of carrier into account, a conversion between the units can be applied (Mook & van der Plicht 1999, Stenström et al. 2011, Hippe & Lifton 2014). For the sampling at day 1'252, the conversion factors for the liquid samples can be specified approximately as follows:

- directly analysed by wet oxidation technique (i.e. d-$TO^{14}C$ and $TI^{14}C$) and pre-treated with an Ag/Ba/H cartridge and analysed by wet oxidation (i.e. p-$TO^{14}C$):

  1 $F^{14}C$ ~ 38 – 40 fM;

- pre-treated with an Ag/Ba/H cartridge, separated by HPIEC and analysed by wet oxidation technique (i.e. ^{14}C-bearing carboxylic acids):

  1 $F^{14}C$ ~ 39 fM.

The conversion factors used for d-$TO^{14}C$, $TI^{14}C$, p-$TO^{14}C$ and ^{14}C-bearing carboxylic acids are slightly different for each sample (see Tab. 15). This is due to the slightly different amount of solution injected (i.e. 125 µL for d-$TO^{14}C$, p-$TO^{14}C$ and $TI^{14}C$ and 9 × 14 µL for ^{14}C-carboxylic acids) and the slightly different amounts of ^{12}C carrier added (target 50 µL) as a result of small variations of the pipetted volume of carrier.

The conversion factors for the gaseous samples are as follows:

- When 500 µL sample volumes were injected in parallel with 50 µg of ^{12}C carrier (i.e. $^{14}CH_4$ and total ^{14}C gas):

  1 $F^{14}C$ = 9.8 fM;

- When 500 µL sample volumes were injected in parallel with 60 µg of ^{12}C carrier (i.e. $^{14}C_2H_6$):

  1 $F^{14}C$ = 11.7 fM.

The conversion factors used for $^{14}CH_4$/total ^{14}C gas and $^{14}C_2H_6$ are different because the amount of the ^{12}C carrier was also different (i.e. 50 µg for the analyses of $^{14}CH_4$/total ^{14}C vs. 60 µg for $^{14}C_2H_6$). The volume of the gaseous sample injected was the same for both analyses and equal to 500 µL.

$TI^{14}C$ was determined to be ~ 244 fM. $TO^{14}C$ was obtained in three different ways: (i) direct measurement by wet oxidation (d-$TO^{14}C$), (ii) after pre-treatment with the Ag/Ba/H cartridge (p-$TO^{14}C$) and as (iii) the sum of the main single aqueous ^{14}C-bearing organic compounds. Direct measurement of the organic ^{14}C content (d-$TO^{14}C$) resulted in the highest ^{14}C concentration (i.e. ~ 803 fM). The organic ^{14}C content after cartridge treatment (p-$TO^{14}C$) was lower (i.e. ~ 522 fM), indicating that a portion of the $TO^{14}C$ was retained by the Ag/Ba/H cartridge (Tab. 15). The

TO^{14}C was estimated at ~ 319 fM by summing up the ^{14}C concentrations of the individual ^{14}C-bearing carboxylic acids identified by CSRA. The uncertainty of the latter measurements is estimated at ~ 30 %. Thus, the TO^{14}C values fairly agree within the estimated uncertainty.

In the gas phase, TG^{14}C was determined to be ~ 56 fM. $^{14}CH_4$ was identified as the main species at an average concentration of ~ 51 fM (Tab. 15). $^{14}C_2H_6$ was present at ~ 1.2 fM, while the speciation of the remaining ^{14}C (~ 3.8 fM) is unknown. With time, the proportion of the ^{14}C inventory in the gas phase is expected to slowly increase in line with the very low corrosion rate of irradiated steel in highly alkaline conditions.

The proportions of ^{14}C in the reactor after 1'252 days of corrosion were as follows: 5 ± 0.3 % of ^{14}C in the gas phase, 22 ± 4 % in the dissolved inorganic chemical form (TI^{14}C) and 73 ± 22 % in the dissolved organic chemical form (TO^{14}C) (Fig. 22b).

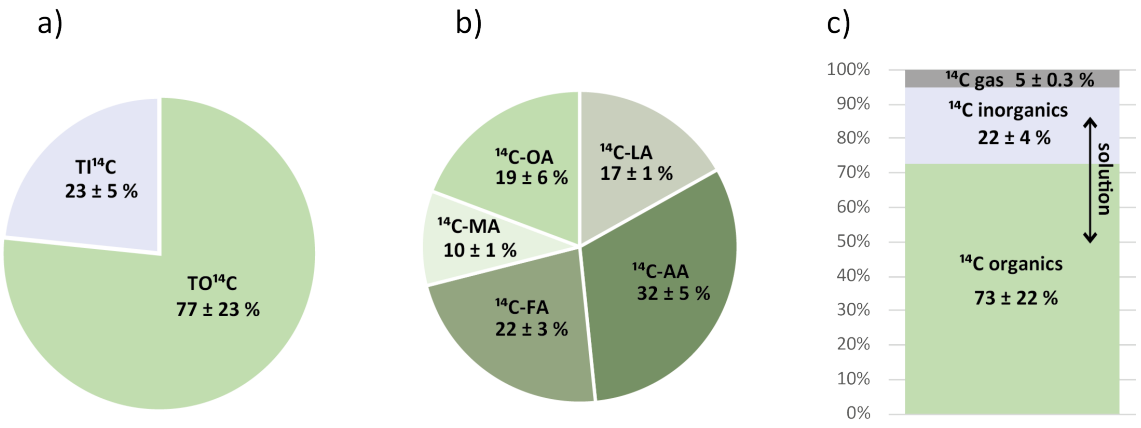

Fig. 22: ^{14}C distribution in the liquid and gas phases of the reactor after 1'252 days of corrosion of irradiated steel in alkaline anoxic conditions: a) Proportions of organic and inorganic ^{14}C, b) proportions of ^{14}C-bearing carboxylic acids in solution, c) proportions of ^{14}C in solution and the gas phase

Tab. 15: $F^{14}C$ values after corrections and calculation of ^{14}C concentrations of the dissolved and gaseous ^{14}C-bearing carbon compounds after 1'252 days of alkaline anoxic corrosion of irradiated steel

Phase	**Samples**	**$F^{14}C$ after corrections** [$F^{14}C$]	**^{14}C concentration** [fM]	**^{14}C concentration average** [fM]	**Error** [%]	**Conversion factor** [fM/$F^{14}C$]
Liquid	LA-1	1.41	53.9	53.6	6	38.2
	LA-2	1.34	53.2			39.7
	AA-1	2.57	98.9	100.8	17	38.5
	AA-2	2.60	102.7			39.5
	FA-1	1.89	73.1	72.0	14	38.7
	FA-2	1.91	70.9			37.1
	MA-1	0.81	31.7	31.3	12	39.1
	MA-2	0.77	30.9			40.1
	OA-1	1.50	59.3	61.4	30	39.5
	OA-2	1.58	63.4			40.1
	Sum CAs			319.1		
	d-TO^{14}C-1	21.86	835.1	802.5	30	38.2
	d-TO^{14}C-2	21.87	769.8			35.2
	p-TO^{14}C-1	13.04	520.3	521.6	30	39.9
	p-TO^{14}C-2	13.17	522.8			39.7
	TI^{14}C-1	6.04	230.7	244.4	2	38.2
	TI^{14}C-2	6.50	258.1			39.7
Gas	CH_4-1	5.32	52.1	51.1	7	9.8
	CH_4-2	5.32	52.1			9.8
	CH_4-3	5.01	49.1			9.8
	C_2H_6-1	0.10	1.17	1.17	20	11.7
	C_2H_6-2	0.11	1.29			11.7
	C_2H_6-3	0.09	1.05			11.7
	Total gas-1	5.62	55.1	56.4	5	9.8
	Total gas-2	5.72	56.6			9.8
	Total gas-3	5.87	57.5			9.8

5 Summary

Information about the speciation of ^{14}C-bearing carbon compounds released during alkaline anoxic corrosion is needed to support the safety assessment of repositories containing irradiated metallic waste. To fill this knowledge gap, a unique corrosion experiment with irradiated steel nut specimens was started in May 2016 and has been running since then at the Paul Scherrer Institute. A specific analytical technique based on very sensitive ^{14}C quantification by AMS was developed as it was expected that the concentrations of the ^{14}C-bearing carbon compounds might be extremely low due to the small ^{14}C inventory of the irradiated steel used for the corrosion experiment and the very low corrosion rate of steel in strongly alkaline conditions.

Several AMS-based methods were developed to determine the total ^{14}C contents in solution and the gas phase: (i) total ^{14}C content associated with organic carbon compounds (d-TO^{14}C, p-TO^{14}C) and inorganic carbon compounds (TI^{14}C), and (ii) total ^{14}C content in the gas phase (TG^{14}C). Furthermore, CSRA was developed for the identification and quantification of single ^{14}C-bearing carbon compounds in the liquid and gas phases. CSRA is based on the chromatographic separation of single compounds by HPIEC of aqueous species and by GC of gaseous species. For CSRA of the gaseous species an oxidation process was involved, which converted HCs into CO_2. The latter species was collected in the sampling loops of a custom-made fraction collector and directly injected into the GIS of the AMS. All methods were tested using standards to determine the efficiency of the involved analytical processes and devices, the recovery rate and the reproducibility of the methods.

The various methods were applied to quantify ^{14}C in the liquid and gas phases sampled from the reactor after 1'252 days of corrosion of irradiated steel. $^{14}CH_4$ was the major ^{14}C-bearing carbon compound present in the gas phase as its concentration agreed well with the total ^{14}C content in the gas phase. $^{14}C_2H_6$ could be a minor species, while its concentration was close to the LOD. The proportion of ^{14}C bound in the organic chemical form in solution was predominant with 77 ± 22 %. TI^{14}C only reached 23 ± 4 %. CSRA of dissolved ^{14}C-bearing carbon compounds showed that ^{14}C-bearing FA and AA are important carbon compounds, thus confirming previous results of Cvetković et al. (2018a). In addition, ^{14}C-bearing OA, MA and LA were identified. Future samplings of the corrosion experiment with irradiated steel will allow us to critically assess the currently available data.

Acknowledgements

Partial financial support for this project was provided by swissnuclear (Project title: "Investigation of the chemical speciation of ^{14}C released from irradiated steel"), the EU project CAST (grant agreement no. 604779), and Nagra. Specific tasks within this project have been developed in co-operation with Brechbühler AG (Schlieren, Switzerland), the commercial partner in the project. The innovative technical developments and the valuable contributions to the project by P. Pichler, Ph. Mottay and B. Oberlin (all Brechbühler AG) are gratefully acknowledged.

6 References

Allard, B., Torstenfelt, B. & Andersson, K. (1981): Sorption studies of $H^{14}CO_3^-$ on some geological media and concrete. Material Research Society Symposium Proceedings 3, 465-473.

Barwick, V. & Prichard, E. (2011): Eurachem guide: Terminology in analytical measurement – Introduction to VIM 3. Available at: www.eurachem.org.

Bayliss, S., Ewart, F.T., Howse, R.M., Smith-Briggs, J.L., Thomason, H.P. & Willmott, A. (1988): The solubility and sorption of lead-210 and carbon-14 in a near-field environment. Material Research Society Symposium Proceedings 112, 33-42.

Cvetković, B.Z., Salazar, G., Kunz, D., Tits, J., Szidat, S. & Wieland, E. (2018a): Quantification of dissolved organic ^{14}C-containing compounds by accelerator mass spectrometry in a corrosion experiment with irradiated steel. Radiocarbon 60/5-6, 1711-1727.

Cvetković, B.Z., Rothardt, J., Buttler, A., Kunz D., Schlotterbeck, G. & Wieland, E. (2018b): Formation of low-molecular-weight organic compounds during anoxic corrosion of zero-valent iron. Environmental Engineering Science 35, 447-461.

Cvetković, B.Z., Salazar, G., Kunz, D., Szidat, S. & Wieland, E. (2018c): Analysis of C-14-bearing compounds released by the corrosion of irradiated steel using accelerator mass spectrometry. Analyst 143/13, 3059-3067.

Diomidis, N. (2014): Scientific basis for the production of gas due to corrosion in a deep geological repository. Nagra Arbeitsbericht NAB 14-21.

Espic, C., Liechti, M., Battaglia, M., Paul, D., Röckmann, T. & Szidat, S. (2019): Compound-specific radiocarbon analysis of atmospheric methane: a new pre-concentration and purification set-up. Radiocarbon 61/5-6, 1461-1476.

Glaus, M.A. & Van Loon, L.R. (2004): A generic procedure for the assessment of the effect of concrete admixtures on the retention behaviour of cement for radionuclides: Concept and case studies. PSI Bericht 04-02, Paul Scherrer Institut, Villigen PSI, Switzerland and Nagra Technical Report NTB 03-09.

Guillemot, T., Cvetković, B.Z., Kunz, D. & Wieland, E. (2020): Processes leading to reduced and oxidised carbon compounds during corrosion of zero-valent iron in alkaline anoxic conditions. Chemosphere 250, 126230.

Hippe, K. & Lifton, N.A. (2014): Calculating isotope ratios and nuclide concentrations for in situ cosmogenic ^{14}C analyses. Radiocarbon 56/3, 1167-1174.

Johnson, L. & Schwyn, B. (eds.) (2008): Proceedings of a Nagra/RWMC Workshop on the release and transport of C-14 in repository environments. Nagra Arbeitsbericht NAB 08-22.

Keith, L-H., Crummett, W., Deegan, J., Libby, R.A., Taylor, J.K. & Wentler, G. (1983): Principles of environmental analysis. Analytical Chemistry 55, 2210.

Kutschera, W. (2005): Progress in isotope analysis at ultra-trace level by AMS. International Journal of Mass Spectrometry 242, 145-160.

Mook, W.G. & van der Plicht, J. (1999): Reporting ^{14}C activities and concentrations. Radiocarbon 41, 227-239.

Nagra (2002): Project Opalinus Clay: Safety report. Demonstration of disposal feasibility for spent fuel, vitrified high-level waste and long-lived intermediate-level waste (Entsorgungsnachweis). Nagra Technical Report 02-05.

Nagra (2014): Modellhaftes Inventar für radioaktive Materialien MIRAM 14. Nagra Technischer Bericht NTB 14-04.

Nagra (2016): Waste Management Programme 2016 of the Waste Producers. Nagra Technical Report NTB 16-01E.

NDA (2012): Geological disposal. Carbon-14 Project – Phase I report. Technical Report NDA/RWMD/092. Nuclear Decommissioning Authority, Harwell Oxford, United Kingdom.

Pointeau, I., Coreau, N. & Reiller, P. (2003): Etude expérimentale et modélisation de la rétention de $^{14}CO_3^{2-}$ par les matériaux constituant le béton dans le cadre des études de faisabilité d'un stockage de déchets graphites. Andra Report FRP 18 CEA 03-001. Andra, Paris, France.

Rauber, M. (2018): Compound-specific radiocarbon analysis of aerosols. Master Thesis, 80 pp, Faculty of Science, Bern.

Ruff, M., Fahrni, S., Gäggeler, H.W., Hajdas, I., Suter, M., Synal, H.A., Szidat, S. & Wacker, L. (2010a): On-line radiocarbon measurements of small samples using elemental analyzer and MICADAS gas ion source. Radiocarbon 52/3-4, 1645-1656.

Ruff, M., Szidat, S., Gäggeler, H.W., Suter, M., Synal, H.A. & Wacker, L. (2010b): Gaseous radiocarbon measurements of small samples. Nuclear Instruments & Methods in Physics Research Section B 268, 790-794.

Salazar, G., Zhang, Y.L., Agrios, K. & Szidat, S. (2015): Development of a method for fast and automatic measurements of aerosol samples by on-line coupling of an elemental analyzer with a MICADAS AMS. Nuclear Instruments & Methods in Physics Research Section B 361, 163-167.

Schumann, D., Stowasser, T., Volmert, B., Gunther-Leopold, I., Linder, H. & Wieland, E. (2014): Determination of the ^{14}C content in activated steel components from a neutron spallation source and a nuclear power plant. Analytical Chemistry 86/11, 5448-5454.

Smart, N.R. (2009): Corrosion behaviour of carbon steel radioactive waste packages: a summary review of Swedish and U.K. research. Corrosion 65/3, 195-212.

Smart, N.R., Blackwood, D.J. & Werme, L. (2002): Anaerobic corrosion of carbon steel and cast iron in artificial groundwaters: Part I- Electrochemical aspects. Corrosion 58/7, 547-559.

Stenström, K.E., Skog, G., Georgiadou, E., Genberg, J. & Johansson, A. (2011): A guide to radiocarbon units and calculations. Internal Report LUNFD6(NFFR-3111), 1-17. Lund University, Sweden.

Swanton, S.W., Baston, G.M.N. & Smart, N.R. (2015): Rates of steel corrosion and carbon-14 release from irradiated steels – state of the art review. CAST WP2 Report Deliverable 2.1. Brussels.

Synal, H.A., Stocker, M. & Suter, M. (2007): MICADAS: A new compact radiocarbon AMS system. Nuclear Instruments & Methods in Physics Research Section B-Beam Interactions with Materials and Atoms 259, 7-13.

Szidat, S., Salazar, G.A., Vogel, E., Battaglia, M., Wacker, L., Synal, H.-A. & Türler, A. (2014): ^{14}C analysis and sample preparation at the new Bern Laboratory for the analysis of radiocarbon with AMS (LARA). Radiocarbon 56/2, 561-566.

Thermo Fisher Scientific (2010): Trace GC Ultra Gas Chromatograph – Operating manual PN31709170, 534 pp. Thermo Fisher Scientific, Rodano, Italy.

Turteltaub, K.W. & Vogel, J.S. (2000): Bioanalytical applications of accelerator mass spectrometry for pharmaceutical research. Current Pharmaceutical Design 6, 991-1007.

Varlet, V., Smith, F. & Augsburger, M. (2013): Indirect hydrogen analysis by gas chromatography coupled to mass spectrometry (GC-MS). Journal of Mass Spectrometry 48, 914-918.

Wacker, L., Fahrni, S.M., Hajdas, I., Molnar, M., Synal, H.A., Szidat, S. & Zhang, Y.L. (2013): A versatile gas interface for routine radiocarbon analysis with a gas ion source. Nuclear Instruments & Methods in Physics Research Section B-Beam Interactions with Materials and Atoms 294, 315-319.

Wieland, E., Cvetković, B.Z., Kunz, D., Salazar, G. & Szidat, S. (2017): Identification and formation of carbon-14 containing organic compounds during anoxic corrosion of activated steel in alkaline conditions. Proceedings of the International High-Level Radioactive Waste Management Conference (IHLRWM) 2017, 9-13 April 2017, Charlotte, USA, 506-511.

Yim, M.-S. & Caron, F. (2006): Life cycle and management of carbon-14 from nuclear power generation. Progress in Nuclear Energy 48, 2-36.